

Molecular Design in Area-Selective Atomic Layer Deposition: Understanding Inhibitors and Precursors

Published as part of *Chemistry of Materials* special issue "Precision Patterning".

Yujin Lee,[§] Amnon Rothman,[§] Alexander B. Shearer, and Stacey F. Bent*



Cite This: *Chem. Mater.* 2025, 37, 1741–1758



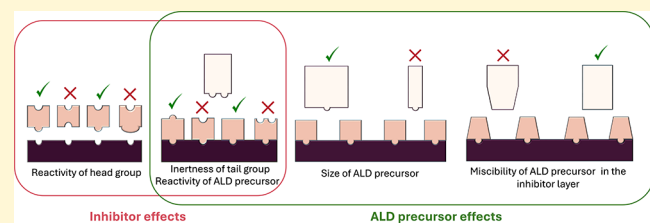
Read Online

ACCESS |

Metrics & More

Article Recommendations

ABSTRACT: Area-selective atomic layer deposition (AS-ALD) has become an essential technique in precision patterning due to its ability to deposit thin films with high conformality and angstrom-level thickness control exclusively in targeted areas. This bottom-up approach offers significant advantages over conventional top-down patterning methods such as photolithography, which encounter challenges like edge placement error and require multiple processing steps. AS-ALD, with its precise control over nanostructure fabrication, supports the development of advanced devices and extends its applications to diverse fields such as sensing, catalysis, and energy. This Review considers molecular design in AS-ALD, highlighting the molecular-level interactions between atomic layer deposition (ALD) precursors and inhibitors with a focus on how variations in precursor ligands and inhibitor head and tail groups influence selectivity. Recent advancements and experimental insights are summarized to provide an understanding of the chemical mechanisms underlying AS-ALD processes. By offering detailed molecular insights, this Review aims to enhance the selection and design of precursor and inhibitor molecules, thereby advancing the development of AS-ALD across various technological fields.



1. INTRODUCTION

Modern electronic devices demand higher speed, lower power consumption, and lower costs, which drive the continued downscaling of device sizes as well as greater 3D integration. These trends toward 3D integration and scaling, in turn, impel the need for innovative fabrication methods. Conventional top-down patterning techniques that rely on photolithography often encounter edge placement error issues at the nanometer scale, which can lead to compromised device characteristics such as short circuits near adjacent electrodes.¹ Moreover, the complexities of the top-down patterning approach require multiple process steps, including repetitive deposition and etching, resulting in considerable time and cost expenditures. For these reasons, there is a growing focus on bottom-up patterning methods as complementary strategies to address these challenges, offering precise control over nanostructure fabrication and potential defect mitigation. Bottom-up fabrication can also enable applications beyond microelectronics, such as sensing, catalysis, and energy.

As a bottom-up approach, area-selective deposition (ASD) stands out for its ability to deposit materials exclusively in targeted regions, offering a viable solution for complicated processes, especially those involving the 3D integration of semiconductor devices.² This method reduces mask requirements compared to traditional top-down photolithography techniques and can simplify the fabrication process by

eliminating the need for a subsequent etch step. ASD methods that selectively deposit thin films only in desired areas can greatly minimize process steps and costs. In addition to these advantages, bottom-up approaches are playing an essential role in the fabrication of next-generation 3D integrated devices, such as gate-all-around field-effect transistors (GAA-FETs).

Achieving area selectivity typically relies on differences in the properties of the material present at different areas on the substrates. This may include not only the chemical properties of materials but also physical characteristics, such as phase, crystal facet, and surface morphology. The method provides a critical contribution to the advanced development of semiconductor technology, particularly in advancing complex 3D integration. Various methods, such as chemical vapor deposition (CVD) and especially atomic layer deposition (ALD), have been extensively explored to achieve ASD.^{3–10} In particular, ALD represents a significant focal point in ASD research. Based on self-limiting reaction mechanisms, ALD

Received: October 18, 2024

Revised: February 6, 2025

Accepted: February 6, 2025

Published: February 20, 2025



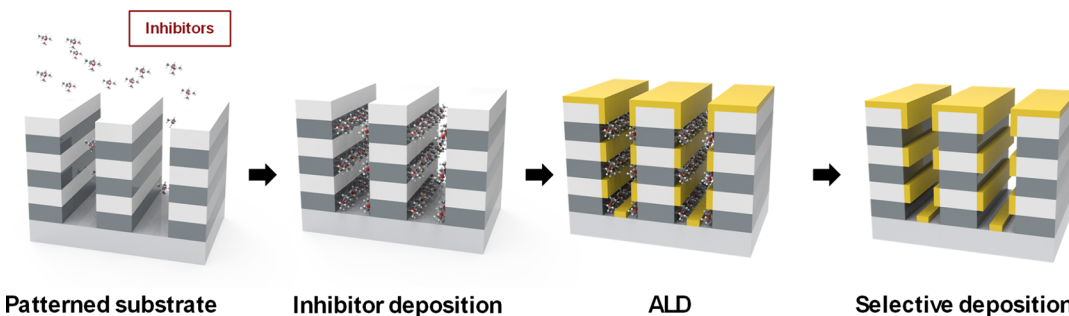


Figure 1. Schematic of the AS-ALD process on a patterned substrate. The illustration demonstrates the selective deposition of thin films on specific regions of a 3D structure, such as might be found in 3D NAND. Example materials relevant to AS-ALD applications in 3D NAND include tungsten (W) or titanium nitride (TiN) for gate stack formation and silicon oxide (SiO_2) or silicon nitride (Si_3N_4) for spacer layers. These applications highlight the importance of achieving high selectivity to minimize processing steps in advanced 3D device architectures.

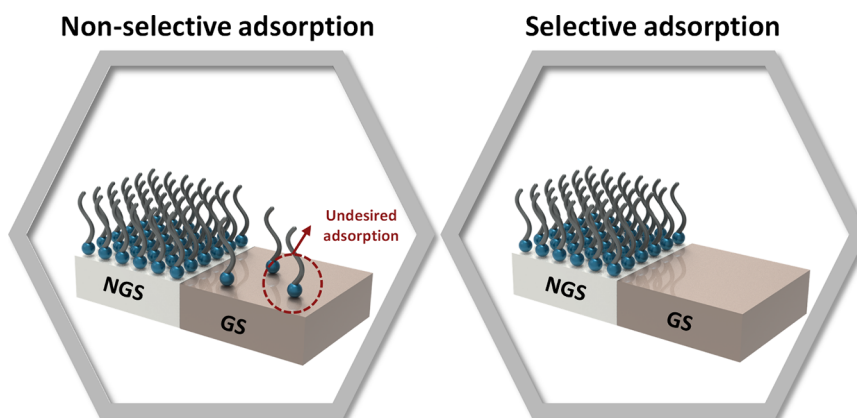


Figure 2. Schematic showing inhibitor–substrate interactions. Selective adsorption of the inhibitor on the NGS is desired. Undesired adsorption of the inhibitor on the GS may interfere with ALD on the GS and lead to reduced selectivity.

alternately introduces two gaseous reagents, the precursor and the counter-reactant, to deposit thin films onto a substrate.¹¹ This unique process affords precise control over film thickness, facilitates the deposition of high-quality thin films with fewer pinholes and defects, and ensures exceptional conformality, making it especially suitable for fabricating 3D-integrated devices and structures requiring lateral uniformity. Therefore, ALD has emerged as the leading method for such applications. Given these promising properties, significant research has been conducted to advance area-selective ALD (AS-ALD) and improve its applicability and performance in semiconductor device fabrication.^{2,6,8,12,13}

AS-ALD has attracted significant attention from both academic research groups and industry due to its versatility and applicability. The implementation of AS-ALD can be broadly categorized into three approaches. The first is an “activation” method that involves creating surface reactive sites where precursors can adsorb in desired areas for thin film deposition (called the growth surface (GS)). The second, the “deactivation” method, removes surface reactive sites to prevent precursor adsorption in nontargeted areas (called the nongrowth surface (NGS)). Finally, the third approach of “inherent” AS-ALD utilizes the unique substrate characteristics to selectively deposit thin films by exploiting intrinsic preferences in precursor adsorption. Of these three approaches, deactivation is widely employed because it effectively amplifies any inherent differences in deposition rate between GS and NGS regions by blocking unwanted precursor adsorption on the NGS, as shown in Figure 1.

Deactivation can be achieved by attaching various species to the NGS, including self-assembled monolayers (SAMs), small molecule inhibitors (SMIs), and polymers. SAMs offer superior selectivity and applicability to various substrates, but wet chemistry is often required due to their low volatility.^{14–17} Moreover, their large size may hinder compatibility with sub-10-nm technologies, particularly in high aspect ratio structures where dense packing is challenging.^{18–20} To address these drawbacks, SMIs have been gaining attention. With higher volatility and smaller size than SAMs, SMIs are better suited for sub-10-nm or 3D structures. In addition, SMIs can be more easily reapplied during the ALD process through the vapor phase, enhancing their utility.^{12,13,21,22} Polymers, which are well established in Si device fabrication, particularly as photoresists (PR) in photolithography, have also been explored for ASD.^{23,24} Unlike SAMs, which form chemical bonds with surface species, polymers typically physisorb on surfaces. Thus, a significant disadvantage of using polymers as inhibitors for ASD is the inability, in most cases, for them to be attached selectively to different surfaces, which limits their effectiveness in more complex patterning applications, although with clever design, polymers can be selectively applied to surfaces by taking advantage of dewetting phenomena.²⁵ Consequently, both SAMs and, more recently, SMIs have received the greatest attention to date in AS-ALD research.

Together with ongoing efforts to explore new inhibitors and their practical application in the AS-ALD process, there is significant interest in understanding the underlying chemical

reactions occurring during AS-ALD. As previously discussed, ALD is based on alternating cycles of precursor and counter-reactant, and AS-ALD relies on specific chemical reactions at the surface. One particularly fruitful approach is to explore and ultimately exploit the interrelationship between the properties of the precursor molecules and those of the inhibitors. For example, surface reactivity can depend strongly on the identity of the ligands and metal center of the ALD precursor, as well as on the inhibitor's molecular properties. Recent studies have provided new understanding by comparing the selectivity across different precursor ligands for the same metal center using a single inhibitor.^{22,26–28} There is now an opportunity to expand further and study the precursor-inhibitor interactions even more systematically. To support this effort, this review aims to provide molecular insights into how precursor ligand types and functional groups within the SAM and SMI inhibitors influence AS-ALD selectivity. We first explain the features of inhibitors and then describe the properties of ALD precursors, offering guidance into selecting suitable molecules for future AS-ALD applications throughout.

2. INHIBITORS

2.1. Introduction to Inhibitors in the ALD Process. In AS-ALD, the role of the inhibitor is to prevent ALD on the NGS. Good coverage of the inhibitor on the NGS facilitates the blocking of ALD, as described below. At the same time, so as not to impede deposition on the GS, it is desirable that the inhibitor adsorb with high selectivity only the NGS, as schematically presented in Figure 2. Unwanted adsorption of the inhibitor on the GS may interfere with ALD on the GS and lead to reduced selectivity. It may also introduce contamination into the deposited film on the GS. Furthermore, if the inhibitor is redosed into the system or sequentially dosed during the ALD process, the inhibitor must not adsorb onto the deposited film's surface, or else it will interfere with continued film growth on the GS. We note that while some degree of inhibitor adsorption on the GS may lead to an initial reduction in growth per cycle, ALD growth can still initiate and eventually reach steady state growth, as long as sufficient growth sites are available on the GS.

Although both SAMs and SMIs are used to inhibit deposition in AS-ALD, there are structural differences between them. SAMs are composed of amphiphilic molecules that include three essential components: a reactive headgroup that facilitates selective binding to the surface, a tail group that renders the film inert to ALD chemistry, and a backbone that supports the formation of a densely packed monolayer through van der Waals forces.²⁹ In contrast, SMIs are smaller molecules, typically on the subnanometer scale, characterized by a chemisorptive reactive group and an inert functional group with minimal intermolecular interactions,¹³ as schematically shown in Figure 3. Although in many cases for SMIs, the entire adsorbate provides both bonding to the substrate and inertness toward the ALD precursor,²⁶ for clarity here we treat the molecular properties of the inhibitors by focusing on their discrete functional groups: the head groups, responsible for reactive interactions with the substrate; the backbone, which impacts packing and interaction with the ALD precursor; and the tail groups, which act as an inert barrier to deposition. For the head groups, the interaction between most inhibitors and the substrate fundamentally involves an acid–base reaction. This necessitates considering the compatibility of the inhibitor's headgroup with the substrate's surface properties

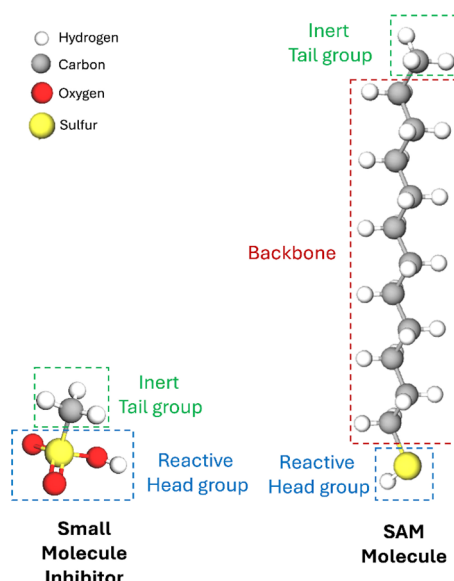


Figure 3. Schematic illustration of example SMI and SAM molecules comparing their functional components: reactive headgroup, backbone (SAM only), and inert tail group.

to ensure effective binding on the NGS. Regarding the tail groups of SMIs, without the ability to achieve the semicrystalline organic regions formed by tightly packed alkyl chains characteristic of SAMs, the primary role of these inhibitors is to prevent the ALD precursor from reacting with the substrate surface. This is achieved by introducing chemical inertness toward the ALD precursor.

Before delving into the role of inhibitors in the AS-ALD process, it is important to address another critical aspect of AS-ALD: the variability in the surface composition of both growth and nongrowth surfaces. This variability can be influenced by factors such as growth conditions, atmospheric exposure, and the overall process scheme. Such variations often necessitate specific surface pretreatments to effectively functionalize the NGS. For example, M. Pasquali et al. recently studied the impact of Cu surface pretreatment on the formation of octadecanethiol-derived (ODT) SAMs used as inhibitors for AS-ALD of hafnium nitride.³⁰ The authors investigated various cleaning procedures, including rinsing with ethanol, dipping in citric acid, dipping in glyoxylic acid, etching the surface with hydrofluoric acid, and simple cleaning with UV ozone. The study found that organic acid-mediated etching of Cu oxide, e.g., with citric acid and glyoxylic acid, significantly limited the formation of the SAM, resulting in a poor ODT layer that was ineffective for ALD inhibition. In contrast, oxidizing pretreatments and cleaning with hydrofluoric acid produced dense organic layers with rapid formation kinetics. Although ODT chemisorption occurred via S–Cu bond formation in all cases, the stability of the ODT layer differed depending on how the substrate was prepared. While this aspect of AS-ALD is undoubtedly important, it is not the primary focus of this review. The following section focuses on the role of inhibitor interactions with the surface and ALD precursors.

2.2. Head Groups. A practical approach to evaluating inhibitor-substrate compatibility is to assess their relative acidities. Generally, inhibitors with strongly acidic adsorption groups tend to interact robustly with basic substrates while interacting more weakly with acidic surfaces.¹³ This relationship highlights how the acidic and basic characteristics of both

Table 1. Summary of Common Types of AS-ALD Inhibitor Head Groups^a

inhibitor's headgroup	chemical moiety	nongrowth surface	growth surface	nature of inhibitor	ref
thiols	R-SH	metals (Cu, Co)	oxides (SiO_2)	acidic	31–38
alcohols and organic acids	R-OH R-C(=O)OH R-S(=O) ₂ -OH R-P(=O)-OH ₂	metals (Cu, Co); oxides (Al_2O_3 , ZnO , TiO_2 , Ta_2O_5 , ZrO_2 , Co_3O_4)	metals (Ru, W); oxides (SiO_2 , TiO_2)	acidic	28, 39–46
β -diketones	R-C(=O)-CH ₂ -C(=O)-R'	oxides (Al_2O_3 , TiO_2 , HfO_2)	oxides (SiO_2 , GeO_2 , WO_3)	acidic	47–50
aminosilanes	R-SiNH ₂	oxides (SiO_2)	H-terminated Si	basic	21, 26, 51
other organosilanes	R-SiCl ₃ R-Si(OCH ₃) ₃	oxides (SiO_2 , Al_2O_3)	H-terminated Si; metals (Cu)	acidic	22, 52–56

^aThese inhibitors are expected to adsorb on the NGS but not on the GS. For the different non-growth and growth surface categories, example substrates are given in parentheses. In the chemical moiety column, examples are given where R and R' designate organic groups.

the adsorbing groups and the substrate surface critically influence the efficacy and strength of the substrate-inhibitor interface interactions. Common head groups of AS-ALD inhibitors are summarized in Table 1 and described further in the sections below.

2.2.1. Thiols. Thiol-based inhibitors contain in their headgroup sulfur atoms, which have a high affinity for metals. The sulfur atom in thiols has lone pairs of electrons, making it an excellent Lewis base that can readily interact with the d-orbitals of metal atoms, facilitating strong coordination bonds and resulting in robust chemisorption. This interaction is especially favorable with metals that possess empty or partially filled d-orbitals.⁵⁷ As a result, thiol or sulfide inhibitors are usually more effective at inhibiting metals than oxides, which form weaker interactions with thiols. A prototypical example of using an inhibitor with a thiol headgroup for a metal/oxide system was recently reported by Lee et al.,³⁴ who used short-chain alkanethiols, such as 1-hexanethiol and 1-propanethiol to selectively deactivate Cu regions relative to SiO_2 regions. One dose of inhibitor successfully blocked up to 200 ALD cycles of Ru ALD, while an ALD-lift-off-redosing sequence blocked up to 300 ALD cycles. Similarly, Chang et al.³² showed a shorter but significant blocking of Al_2O_3 ALD on Co relative to SiO_2 up to 40 ALD cycles using 1H,1H,2H,2H-perfluorodecanethiol (FDT) as an inhibitor. A recent theoretical report by Clerix et al. studied the structure, energetics, and coverage of thiolate SAMs on Cu surfaces.³³ They demonstrated that surface saturation of shorter chain thiolates ($n = 1, 2$) is primarily constrained by steric hindrance. In contrast, longer chain thiolate SAMs ($n = 6, 12$) undergo a phase transition from lying parallel to the copper surface at low coverages to forming tightly packed, upright structures at full surface saturation, following the well-known behavior of self-assembled monolayers.³³

Interestingly, whereas thiols are used most commonly to block metals such as Cu, the application of thiols to the blocking of metal oxides was recently presented. Bergsman et al.³¹ studied the vapor-phase reaction of a dodecanethiol (DDT) SAM with a bare Cu surface to create a stable monolayer that can block some ALD processes. Surprisingly, the reaction of DDT with an oxidized CuO surface led to Cu-thiolate multilayers several nanometers in thickness composed of well-order crystallites oriented parallel or perpendicular to the substrate surface; that multilayer could block up to ~ 7 times more ZnO ALD than could monolayer DDT.³⁵

Various factors can influence the blocking efficiency of thiol inhibitors. Hashemi et al. compared the blocking of metal Cu surfaces by both vapor-deposited and solution-deposited alkanethiol SAMs. Their results demonstrated that a vapor-deposited alkanethiol SAM was more effective in blocking the deposition than a solution-deposited SAM, even after only 30 s of vapor exposure.³⁷ In a different report by Lee and co-workers, the passivation of multiple surfaces using a single inhibitor was achieved when diethylsulfide (DES) was selectively adsorbed on Cu and SiO_2 at high temperatures, resulting in AS-ALD only on the TiN surface.³⁸ The authors showed that DES could undergo dissociation at the Cu surface upon high-temperature exposure, and its subsequent fragments could adsorb onto the SiO_2 substrate while avoiding adsorption onto TiN. Passivation on the SiO_2 surface by the ethyl fragment and release of an ethanethiolate fragment from SiO_2 were deemed the most likely mechanism, whereas strong adsorption of the ethanethiolate fragment was observed on the Cu surface.

2.2.2. Alcohols and Organic Acids. As reactive head groups for inhibitors, alcohols and organic acids have been found to block ALD on both metals and oxides, depending on the interaction of the inhibitor with the substrate. Recent work by Yarbrough et al. used methanesulfonic acid (MSA) as an inhibitor for the selective deactivation of Cu surfaces relative to SiO_2 , TiO_2 , Ru, and W, upon which MSA exhibited much less chemisorption, for AS-ALD of Al_2O_3 .²⁸ The reactive functional group in sulfonic acid contains lone pairs on the oxygen atoms as well as a strongly acidic hydroxyl group. While the hydroxyl group allows chemisorption through a condensation reaction pathway, the lone pairs can interact in a donor–acceptor fashion, particularly with the empty d-orbitals of the metal surface. The high selectivity of MSA was attributed to the surface alkalinity of the native CuO, the ability of MSA to reduce the uppermost layers of this oxide, and the favorable interactions between lone pair electrons from sulfonyl groups in MSA and empty d-orbitals at the resultant copper surface. CuO is the least acidic compared to the other studied substrates and showed the best affinity for MSA.

Similar results were obtained when passivating Cu and Co using octadecylphosphonic acid (ODPA) SAMs as well, enabling selective deposition of dielectric on dielectric (DoD), e.g., Al_2O_3 on SiO_2 without growth on the adjacent metal.³⁹ Interestingly, the same ODPA SAM was used as an inhibitor on various metal oxide surfaces by changing the SAM solvent, to achieve AS-ALD on patterns of chemically similar

dielectric materials.⁴⁵ Under a toluene solvent system, ODPA formed a well-packed SAM structure on Al₂O₃, HfO₂, TiO₂, and Ta₂O₅ but not on native SiO₂ surface, and as a result, ZnO ALD was blocked on those metal oxides and selectively deposited on SiO₂.

Hydroxyl moieties can be found in the head groups of different types of inhibitors besides acids, such as alcohols. Li et al.⁴⁴ used both experiments and random sequential adsorption (RSA) simulations to study the packing of SMIs on a surface in the context of SiO₂ AS-ALD by reapplication of alcohols such as methanol, ethanol, isopropanol, 1-propanol, and 1-butanol prior to every ALD cycle to deactivate an Al₂O₃ surface. They showed that hydroxyl groups of the alcohols interact with the Al₂O₃ substrate surface through hydrogen bond interactions with hydroxyl groups on the partially hydroxylated Al₂O₃ surface. This interaction was the most favorable adsorption mechanism, leading to additional stabilization of the adsorbed molecules and effective precursor blocking during the ALD process. The RSA simulations and density functional theory (DFT) calculations pointed to ethanol as the SMI with the highest efficacy in blocking the oxide surface, mainly attributed to the size and shape of the inhibitor, its reaction with the surface, and its diffusion on the substrate to create a densely packed layer.

Carboxyl groups preferentially adsorb on metal oxide surfaces containing OH groups; adsorption is more favorable on metal oxides with more basic OH groups than those with acidic OH groups. Karasulu et al. studied the area-selective-spatial-ALD of SiO₂ on ZnO as the NGS and SiO₂ as the GS, using two different carboxylic acids as SMIs: ethylbutyric acid and pivalic acid.⁴² By doing interval exposures to the SMI and back-etch correction steps, they could grow up to 23 nm of SiO₂ on the GS, with no deposition on the NGS. Similar to the use of β -diketone inhibitors, which are discussed in the next section, the lower calculated surface acidities of ZnO (1.15 on Sanderson's acidity scale⁴¹) and other metal oxides, such as Ta₂O₅ (2.28) and ZrO₂ (1.07), correlated with the high chemisorption of carboxylic acids and the significant nucleation delay observed for the deposited material on these nongrowth metal oxides. These values emphasize the preferred adsorption and potential blocking of carboxylic acids on more basic surfaces than acidic ones, such as SiO₂ which has a higher Sanderson's acidity scale value of 2.73. In addition, DFT calculations revealed that thermodynamic factors predominantly govern the selective surface functionalization by both carboxylic acids.⁴² The superior selectivity observed with pivalic acid compared to ethylbutyric acid was attributed to its higher packing density.

Carboxylic acids can also be used as SAMs to deactivate metal oxide surfaces.^{40,43} Interestingly, Satyarthi et al. recently reported the use of stearic acid SAM to block CuO and CoO during ZnO deposition and showed nucleation inhibition for up to 25 and 50 cycles on CuO and CoO, respectively.⁴⁶ The results indicated that the CuO and CoO surfaces were not etched, as evidenced by a clear oxygen XPS peak observed on the bare metal surfaces, suggesting the presence of a thin metal oxide layer. Considering this, the calculated Sanderson's acidity values for CuO and CoO of approximately 1.5,⁴¹ which indicate more basic surface characteristics, suggest that the basicity of CuO and CoO enable the chemisorption of the acidic carboxylic groups of the inhibitors.

2.2.3. β -Diketones. The use of β -diketones as SMIs was recently introduced, focusing on acetylacetone (Hacac) and

2,2,6,6-tetramethyl-3,5-heptanedione (Hthd) to deactivate metal oxides.^{47,49} Mameli et al. studied the use of Hacac as an inhibitor, specifically when reapplied every ALD cycle, and presented a 20-cycle ALD SiO₂ delay on Al₂O₃, TiO₂, and HfO₂ as NGS compared to SiO₂, GeO₂, and WO₃ as GS.⁴⁷ As a β -diketone, Hacac can act as a bidentate ligand, which means it can donate electron pairs from both oxygen atoms to the metal center of the substrate. The Hacac exhibits weak acidic properties due to its poor ability to lose a proton and, therefore, mainly binds as a Lewis base. The attachment mechanism involves Lewis acid–base interactions where the metal cations on the surface (e.g., Al³⁺) act as Lewis acids, and the oxygen atoms in Hacac act as Lewis bases. The strong electron-accepting ability of the metal cations forms a stable chelate complex with the Hacac ligand, which donates its lone pairs of electrons to form a stable ring structure on the surface. Hence, the chemisorption of Hacac on the Al₂O₃ surface is favored due to the strong Lewis acid–base interactions between the Lewis acidic sites on Al₂O₃ and the Lewis basic sites on Hacac. In contrast, the SiO₂ and GeO₂ surfaces lack the necessary acidity and suitable surface sites for effective interaction with Hacac, resulting in no significant chemisorption. A follow-up study by the same group compared the use of Hthd and Hacac, as well as acetic acid, as inhibitors for the same material system and found a higher nucleation delay of SiO₂ ALD on Al₂O₃ when Hthd was in use due to higher steric shielding and chemical passivation of the inhibited surface.⁵⁰ Balasubramanyam et al. presented for the first time the use of Hacac as an inhibitor for AS-ALD of a 2D material like WS₂.⁴⁸ An ALD WS₂ nucleation delay of up to 30 cycles was achieved by using Hacac as an inhibitor on Al₂O₃, HfO₂, and TiO₂ as the NGS, compared to SiO₂ as the GS.

In addition to their role as inhibitors, β -diketones like Hacac and Hthd are also commonly used as ligands in ALD precursors, such as metal(acac) and (hfac) compounds. These small molecule byproducts of ALD reactions can contribute to either intentional or unintentional surface inhibition. For example, residual β -diketone fragments might temporarily passivate the surface or compete with the primary SMI, potentially influencing the nucleation delay and overall growth selectivity. Understanding the role of β -diketones as both SMIs and precursor byproducts highlights the inherent complexity of acid–base interactions in AS-ALD systems and underscores the importance of controlling precursor chemistry for effective selective deposition.

Understanding the acid–basic reaction using β -diketone inhibitors can help explain which surfaces support the chemoselective adsorption of Hacac inhibitors and hence provide a nucleation delay and ALD blocking, and which lead to immediate deposition by ALD. Figure 4 from a previous study presents calculated surface acidities for the different starting oxide surfaces.⁴⁷ The vertical line divides the materials depending on whether immediate growth or a nucleation delay is observed, correlated closely with their surface acidities.

2.2.4. Aminosilanes. Short-chain aminosilanes, traditionally used as ALD precursors for SiO₂ thin films, have recently been utilized as SMIs for AS-ALD. These inhibitors can form strong, stable bonds with specific surface groups, particularly hydroxyl groups on oxide surfaces, creating a passivation layer that prevents further reaction or deposition of the ALD precursors. Khan et al. employed short-chain aminosilane precursors as selective inhibitors for AS-ALD.²¹ Bis(N,N-dimethylamino)-dimethylsilane (DMADMS) and (N,N-dimethylamino)-

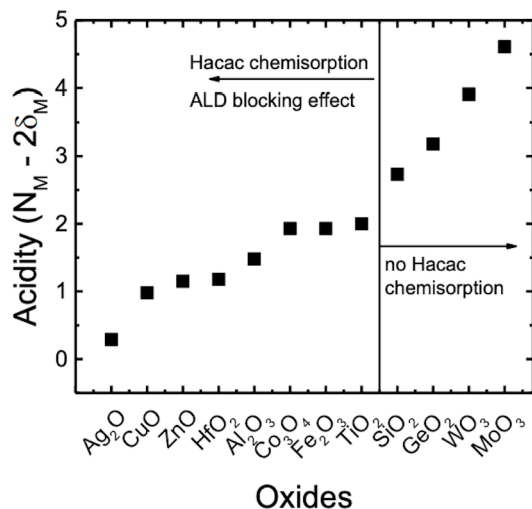


Figure 4. Surface acidity for diverse metal oxides, calculated following the method described by Mameli et al. in ref 47. Reproduced from ref 47. Copyright 2017 American Chemical Society. This publication is licensed under CC-BY-NC-ND.

trimethylsilane (DMATMS) were used to deactivate a SiO₂ surface, compared to a H-terminated Si surface, toward subsequent AS-ALD of Ru and Pt metal on the H-terminated Si GS. Using experimental and theoretical methods, the authors suggested that both DMADMS and DMATMS molecules react with the OH groups on the Si surface, forming Si-CH₃ moieties which block the subsequent ALD precursor. The employed SMIs blocked the growth of Ru up to 100 Å and Pt up to 18 Å, with nucleation delay of 100 and 25 ALD cycles, respectively, although blocking was poorer against Al₂O₃ and HfO₂ ALD. Additionally, as a proof-of-concept, the authors showed the use of the aminosilane SMIs for AS-ALD on nanostructures by growing Ru metal on a MoS₂ flake and not on the surrounding SiO₂ wafer. Similar results of blocking Ru ALD on SiO₂ and SiN were achieved by using (N,N-diethylamino)trimethylsilane (DEATMS).⁵¹

Lee et al. recently demonstrated the use of a different aminosilane molecule, namely di(isopropylamino)silane (DIPAS), to successfully block HfO₂ on SiO₂ as the NGS and allow growth on TiN as the GS, with up to 87% selectivity at 20 ALD cycles.²⁶ In contrast to the use of DMADMS and DMATMS, it was suggested that DIPAS changes the wettability and reactivity of the surface by leaving –SiH₃ species after adsorption, introducing a carbon-free inhibitor that may lead to less cross-contamination. This study and previous studies reveal the importance of choosing suitable inhibitors and ALD precursors in parallel to achieve effective selectivity, as will be discussed further in *Part II*. The authors observed that HfO₂ ALD with hafnium tert-butoxide (Hf(O*t*Bu)₄) or hafnium tetrachloride (HfCl₄) precursors was inhibited on the –SiH₃ terminated SiO₂ substrate formed by DIPAS treatment, whereas HfO₂ ALD using tetrakis(dimethylamido)hafnium (TDMAHf) was not.

2.2.5. Other Organosilanes. Organosilane inhibitors are molecules that contain a silane group (Si-X, where X is usually a halogen or alkoxy group) that reacts with the surface, often an oxide, to form a covalent bond. These linkages can create a stable and well-ordered monolayer. The stable layer can block the interaction between the ALD precursor and the substrate surface, leading to selective deposition. In early AS-ALD work,

Chen et al. used octadecyltrichlorosilane (ODTS) molecules to adsorb selectively on OH-terminated SiO₂ regions, as NGS, compared to H-terminated Si regions, as GS, on the same substrate, allowing for AS-ALD of HfO₂.⁵² The trichlorosilane group in ODTS reacted readily with the surface hydroxyl groups and formed strong covalent Si–O–Si bonds, anchoring the ODTS molecules to the surface.⁵⁶ The advantage of ODTS as a liquid SAM was presented later in several reports as part of microcontact printing to block ALD of Pt, HfO₂, Ir, and TiO₂⁵⁴ on SiO₂ surfaces.

In a different report, Chen et al. studied the effect of various characteristics of organosilane SAMs on blocking ALD of HfO₂ on SiO₂ surfaces.⁵³ The authors expected that the reactivity of Si-X reactive group (where X is Cl, Br, or I atoms in chlorotrimethylsilane, bromotrimethylsilane, and iodotrimethylsilane SAMs, respectively) toward the hydroxyl groups on the substrate surface would increase as the electronegativity of the halogen atom decreases, due to weaker bond strength with the Si atom, but surprisingly their experimental results did not reveal a significant difference in reactivity under the reaction conditions. Their study also focused on the combined effect of other characteristics of the SAMs, such as tail group and tail length, on the reactivity toward the substrate surface and subsequent ALD blocking, as is discussed in the next section.

Another type of organosilane inhibitor commonly used is that of alkoxy silanes. This headgroup has been used in SAMs as well as SMIs. Yarbrough et al. studied methoxysilanes, particularly trimethoxypropylsilane (TMPS), as inhibitors to confer selectivity between Cu as a GS and SiO₂ as NGS for ALD of Al₂O₃.²² The selective inhibition was explained by the presence or absence of proton-donating groups on the surface. While the NGS SiO₂ has acidic hydroxyl groups that can donate a proton to hydrolyze the methoxy groups of the inhibitor, the metallic NGS, like Cu, does not have proton-donating groups. The report also studied the effect of other trifunctional silanes, namely trimethoxymethylsilane (TMMS) and trimethoxyethylsilane (TMES), as well as different Al precursors to identify the most selective Al₂O₃ AS-ALD system supported by this type of inhibitors and is also discussed in depth in the next sections of this review.

2.2.6. General Headgroup Considerations. As explained below, the use of inhibitors in AS-ALD generally functions by deactivating surface reactive sites and replacing them with inert termination groups. While this is true for SAMs, small molecule inhibitors SMIs present additional complexity. Specifically, after interacting with the surface, the remaining activity of the head groups requires further consideration. The nature of the interaction can significantly impact the extent of deactivation. In some cases, the headgroup may still retain some reactive moieties, potentially making it prone to subsequent attack by ALD reactants, especially if the inhibitor does not fully saturate the surface or if the packing density of the SMI is not complete. In other cases, the level of passivation will depend on the stability of the bond formed with the surface. While covalent binding typically leads to a more stable, less reactive attachment, there may be cases where the headgroup can undergo further reactions with ALD precursors, depending on the reactivity of the surface or the ALD reactants used. Therefore, in the limit of headgroup-only SMIs or less-than-perfectly dense packing of inhibitors, it is important to assess the level of deactivation achieved and what remaining surface activity may persist. A key challenge in these systems is determining how much of the surface remains reactive for

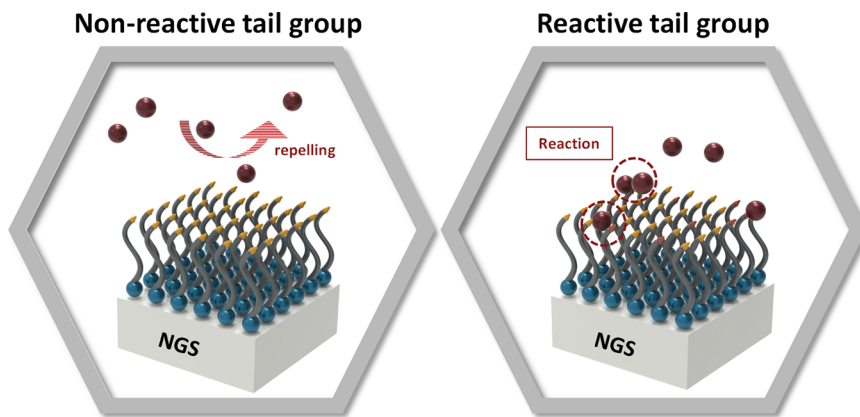


Figure 5. Schematic of the reaction between the tail group and ALD precursor. In the left image, the tail groups are nonreactive, and the ALD precursor does not react with the inhibitor. In the right image, the tail groups undergo a reaction with the ALD precursor.

subsequent ALD cycles and to what extent the remaining activity of the headgroup could influence deposition behavior.

2.3. Backbone and Tail Groups. Inhibitors in AS-ALD generally function by deactivating surface reactive sites and replacing them with inert termination groups, to prevent undesired interactions at the inhibitor-precursor interface, as presented schematically in Figure 5. Two important aspects of the blocking mechanism are the following. First, the reaction of the inhibitor headgroup with surface active sites at the substrate leads to deactivation or removal of those functional groups that would otherwise serve as reactive sites for ALD precursor chemistry. Second, the inhibitor's tail should form a layer that restricts precursor access to any remaining active sites at the underlying substrate. Both mechanisms are important because it is unlikely that all surface reactive groups will be removed by reaction with the inhibitor (step 1), and therefore, those sites that have not been reacted must be protected by access from the ALD precursors by the typically hydrophobic backbone and tail of the inhibitor. Another consideration of the tail group is that the tail should itself be inert to reaction with the ALD precursors.

The previous section focused on the headgroup chemistry, and here we focus on the tail group. The backbones and tail groups of inhibitors in AS-ALD are typically organic C_xH_y species that impart hydrophobic character to the surface. Inhibitors can be especially effective if they minimize defect sites, such as pinholes or loosely packed regions, to more effectively prevent access to the underlying substrate. The performance of SAM inhibitors, for instance, is mainly attributable to their backbone type and length and the ability to form semicrystalline regions, which block the interstitial spaces that facilitate undesired access by the ALD precursor to the substrate below. Conversely, due to their short length, SMIs present a different challenge; degradation of the blocking can occur due to interactions between the ALD precursor and the inhibitor or the underlying substrate. This section reviews the effect of different parts of the tail, such as the backbone type, tail length, and tail groups, on the selective deposition.

2.3.1. Backbone Type. Certain backbone types of inhibitors, usually in the form of SAMs, promote the formation of a densely packed monolayer through van der Waals dispersion forces.^{13,39} In SAMs, the backbones are usually long aliphatic hydrocarbon chains but can also include fluorocarbons^{58–60} and aromatic chains.^{61–64} Traditionally, aliphatic SAMs have been used as inhibitors for AS-ALD due to their ease of

synthesis and application as well as their good packing characteristics. These inhibitors provide good surface coverage because the flexible chains can pack closely together, exhibiting moderate to good hydrophobicity, which effectively blocks many ALD precursors.^{65,66} The chain length of aliphatic SAMs is an important characteristic that determines their effectiveness in blocking ALD precursors, as discussed in the next section.

By modifying the hydrocarbon chain of SAMs, one can create an alternative backbone type consisting of fluorinated carbons. The highly electronegative fluorine atoms create strong C–F bonds, leading to unique surface properties, exceptional chemical resistance, and high stability under a wide range of chemical and thermal conditions.⁶⁷ Fluorocarbon SAMs also provide high hydrophobicity and oleophobicity, making them effective at blocking a wide range of ALD precursors. Early work by Chen et al. compared hydrocarbon alkyltrichlorosilane to fluoroalkyltrichlorosilane SAM deposition on SiO_2 .⁵³ They found that due to the higher reactivity of the fluorine atoms, the SAM is more reactive and becomes denser and more hydrophobic. As a result, fluorocarbon tail chain molecules can provide ALD inhibition similar to that of a hydrocarbon chain molecule but can achieve it with a shorter chain length.⁵³ More recently, Chang et al. compared the use of decylphosphonic acid (C10PA) and the 1H,1H,2H,2H-perfluorodecylphosphonic acid (FC10PA) for AS-ALD of Al_2O_3 on cobalt as nongrowth surface and SiO_2 as the growth surface.⁶⁰ The FC10PA SAM-modified substrates exhibited better blocking ability than the C10PA SAM due to the low surface free energy and amphiphobic property of the fluoroalkyl chain, leading to a nucleation delay of up to 20 ALD cycles. Even compared to an ODPA SAM with its longer 18-carbon alkyl chain, the FC10PA SAM still demonstrated better ALD blocking results against Al_2O_3 ALD deposition. The same research group also recently showed similarly improved blocking of Al_2O_3 ALD using the fluorothiol SAM, 1H,1H,2H,2H-perfluorodecanethiol (FDT) compared to the reference 1-decanethiol (DT) on cobalt and SiO_2 patterned substrates.⁵⁹

Aromatic backbone-containing AS-ALD inhibitors are a less-explored type that show promise due to their ability to interact strongly with certain surfaces, such as metals, while not interacting with others, such as oxides. Aromatic molecules have been shown to block ALD precursor molecules in some systems.⁶² A recent study by Merkx et al. demonstrated the use

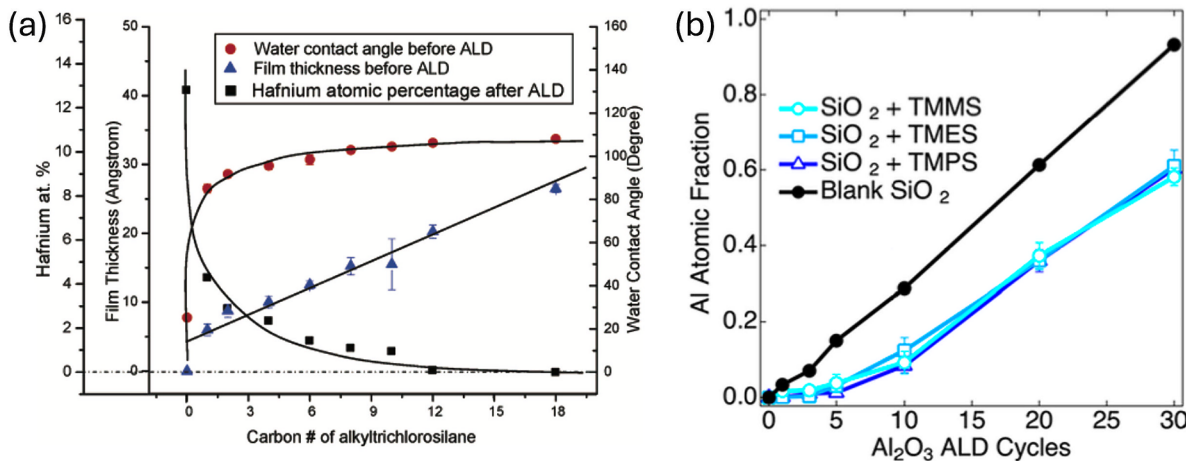


Figure 6. Effect of chain length of SAMs and SMIs. (a) Chain-length dependence of alkyltrichlorosilane SAM blocking efficiency. The plot shows the water contact angle and film thickness before HfO_2 ALD and hafnium atomic percentage after the ALD process as a function of the number of carbon atoms in the SAM tail group. Reproduced from ref 53. Copyright 2005 American Chemical Society. (b) Aluminum atomic fractions from Al_2O_3 ALD on SiO_2 , passivated with trifunctional silane SMIs of varying alkyl chain lengths Reproduced from ref 22. Copyright 2022 American Chemical Society.

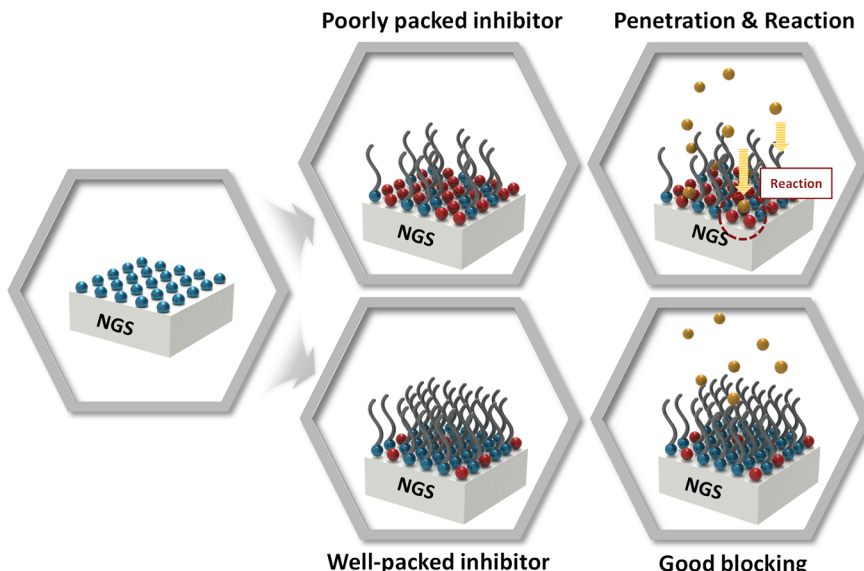


Figure 7. Schematics of the effect of inhibitor layer packing on the penetration of ALD precursor and its blocking ability. A poorly packed inhibitor layer (top series) can lead to penetration and reaction of ALD precursors; a well-packed inhibitor layer (bottom) can prevent access by ALD precursors to reactive sites at the substrate. The blue, red, and orange spheres represent the NGS reactive sites, the unreacted surface sites after applying the inhibitor, and the precursor molecules, respectively.

of aniline as an SMI for the AS-ALD of TiN, blocking growth up to 6 nm on metals such as Co and Ru, which served as the NGS, while allowing TiN deposition on a dielectric GS such as SiO_2 and Al_2O_3 .⁶² The authors hypothesized that because aromatic groups are a common ligand motif for ALD precursors, and those reactions are known to be self-limiting, precursor adsorption should be blocked by surface aromatic groups. On the other hand, despite the effective blocking by an aniline SMI on metal surfaces, a study of a different type of aromatic inhibitor, phenylphosphonic acid (PPA),⁶³ did not show significant enhancement in blocking ability over the reference alkyl inhibitor, octadecylphosphonic acid; rather, the blocking by PPA was significantly worse. This result is consistent with a study of SAM inhibitors that showed poorer blocking when using an aromatic tail compared to a long-chain aliphatic tail.⁵³ The poor blocking in that study was attributed

to the inability of the phenyl rings to form a close-packed film; in addition, the orientation at the substrate was not sufficient for the phenyl rings to achieve $\pi-\pi$ stacking. Thus, the literature suggests that whereas aromatic tail groups may not be effective for SAM-based inhibitors, aromatic molecules can be successfully used as SMIs.

The choice between aliphatic-, aromatic-, and fluorocarbon-containing backbone inhibitors for AS-ALD applications depends on the specific requirements for thermal stability, chemical resistance, inhibition efficiency, and the nature of the substrate and precursor. Each type offers unique advantages that can be tailored to meet the demands of various selective deposition processes.

3.2. Tail and Backbone Length. One of the major factors affecting the deactivation of ALD, especially in the case of SAM inhibitors, is the quality of packing. A long-chain

molecule produces higher van der Waals forces than a short-chain molecule, resulting in denser packing of the long-chain inhibitors. Previous studies have shown that the degree of order of SAMs is strongly dependent on the coverage and the chain length of the backbone.^{68,69} Chen et al. focused on the effect of alkyl chain length of SAMs and demonstrated that increasing the SAM chain length led to a higher degree of packing, as inferred by the water contact angle, which in turn led to increased selectivity in AS-ALD.⁵³ The authors studied a series of *n*-alkyltrichlorosilanes of chain lengths ranging from 1 to 18 carbon atoms as SAMs, and found that longer chain alkyltrichlorosilanes, which are known to form more well-packed SAMs, provided better inhibition of HfO₂ ALD on SiO₂ surfaces. The data showed that when the alkyl chain contains at least 12-carbon atoms, the monolayer converts the surface wetting property to hydrophobic, and the water contact angle does not increase further with increasing chain length, as shown in Figure 6(a).

However, the effect of chain length on blocking efficiency may be different for SMIs. Yarbrough et al. studied a series of trifunctional silanes—TMMS, TMES, and TMPS—and different Al precursors to identify the most selective Al₂O₃ AS-ALD system enabled by these SMIs.²² It was shown that all three of the SMI-treated samples displayed a short nucleation delay and, importantly, that switching from methyl to ethyl to propyl blocking groups showed negligible differences in Al content up to 30 cycles of ALD, as presented in Figure 6(b). Interestingly, Yu et al. recently studied the inhibition of SiO₂ ALD on Al₂O₃ substrates by comparing three SMIs of different sizes—acetic acid (HAc), Hacac, and Hthd—and observed different trends.⁵⁰ Using density functional theory and random sequential adsorption simulations, the authors showed that varying the size of SMIs brings benefits from either higher steric shielding or better chemical passivation. Compared to Hacac, HAc performs better due to its smaller size, yielding denser packing and, thus, higher chemical passivation. Hthd, on the other hand, benefits from its bulkiness with a higher contribution from steric shielding.

An explanation for the discrepancy between SAMs and SMIs in the role that tail length plays has been suggested and is largely attributed to differences in the inhibitor-type blocking mechanisms.^{8,13} SAMs inhibit deposition by a 2-fold mechanism: first deactivating reactive groups, and then reducing the diffusion of precursors through the SAM tails to the substrate surface, as illustrated schematically in Figure 7. In contrast, the smaller size of SMIs primarily limits their blocking mechanism to deactivating surface reactive sites, with less impact on preventing precursor access to the substrate. Consequently, the size of the SMI blocking tail does not affect the blocking performance in the same direct way as SAMs.

2.3.3. Tail Functional Group. The presence of an inert tail group on the inhibitor that does not react with the ALD precursor is crucial to preventing undesired deposition on the nongrowth surface. One of the most common unreactive tail groups is the methyl moiety, which has been used as a termination for most SAMs due to its inertness to a wide variety of chemistries. Xu et al. were the first to study theoretically a comparison of ALD of Al₂O₃ on SAM-terminated SiO₂ with different functional groups such as —CH₃, —NH₂, and —OH.⁷⁰ The calculations showed that the reaction of trimethylaluminum (TMA) and the OH-terminated SAM is favored both thermodynamically and kinetically over the reaction with NH₂- and CH₃-terminated

SAMs. In the case of the CH₃-terminated SAM, there was no thermodynamic driving force for the reaction, and the reaction barrier was ~40 times larger compared to the OH-terminated SAM, preventing reaction with the TMA. Similar results were reported experimentally for blocking titanium ALD precursors on CH₃⁻, NH₂⁻, and OH-terminated SAMs deposited on SiO₂.^{71,72} Patwardhan et al. studied both theoretically and experimentally different types of tail functional groups and compared long alkyl chain SAMs as inhibitors, including —OH, —COOH, and —SH terminations.⁷³ They found that both the carboxylic-acid-terminated and the hydroxyl-terminated SAMs allowed partial nucleation of the deposited material when using diethylzinc (DEZ) or TMA as ALD precursors.

The different blocking behavior for the studied tail functional groups has been explained by comparing the number of lone pair valence electrons that each contains.¹³ The —CH₃ group presents no lone pairs, —NH₂ has one lone pair on the nitrogen atom, —SH has two lone pairs on the sulfur atom, —OH has two lone pairs on the oxygen atom, and —COOH has four lone pairs: two on the carbonyl oxygen atom and two on the hydroxyl oxygen atom. The reactivity of termination groups with ALD precursors, such as TMA or DEZ, is significantly influenced by the number and effectiveness of lone pairs on the atoms in these groups. The —CH₃ group, with no lone pairs, exhibits very low reactivity. The —NH₂ group, with one lone pair on nitrogen, shows moderate to high reactivity due to its ability to act as a Lewis base. The —SH group, with two lone pairs on sulfur, has moderate reactivity. The —OH group, with two lone pairs on oxygen, is highly reactive due to its strong interaction with the ALD precursor. The —COOH group exhibits very high reactivity with two lone pairs, making it highly effective in forming bonds with the ALD precursor. Thus, reactivity increases with the availability and effectiveness of lone pairs, especially on more electronegative atoms.¹³

2.4. Extending the Efficacy of the Inhibitor. As discussed in the previous sections, proper selection of the inhibitor's head and tail groups can lead to desired selectivity. However, it is important to note that the selectivity of an area-selective ALD process eventually diminishes after a certain number of cycles, often due to the degradation of the inhibitor layer. This degradation may occur through the thermal desorption of the inhibitor, interactions between the inhibitor and the precursor, or interactions by reactive counter-reactants. Overcoming the inhibitor's degradation and maintaining selectivity for high ALD cycle numbers has been achieved by different approaches, two of which we highlight here. The first one is regenerating the inhibition layer by redosing the inhibitor molecules repeatedly during the process. Hashemi et al. used this approach by redosing alkanethiol SAMs every 150 ALD cycles and showed the extended nucleation delay of ZnO on the Cu surface, compared to a single dose of the inhibitor at the beginning of the process.^{37,74} Mameli et al. demonstrated a more rigorous use of this approach by redosing the Hacac inhibitor every ALD cycle for selective deposition of SiO₂ on GeO₂, SiN_x, SiO₂, and WO₃ in the presence of Al₂O₃, TiO₂, and HfO₂ surfaces.⁷⁵

While more frequent doses of inhibitors can enhance selectivity, in some systems reapplying the inhibitors can cause cyclic nucleation delays on the GS without eliminating the unwanted material deposited on the NGS. Moreover, once some deposition of material occurs on the NGS, it can be more difficult for the inhibitor to readsorb, as the surface species at

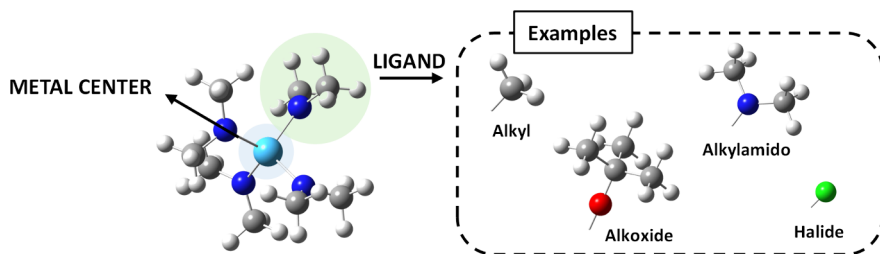


Figure 8. Examples of ALD precursors for thin film deposition. The properties and reactivity of the precursor are a strong function of both the metal center and the ligands. Here, examples of common ligand types are shown. In the ligand, the white, gray, blue, red, and green spheres represent the hydrogen, carbon, nitrogen, oxygen, and halogen atoms, respectively.

the NGS become dominated by the ALD material rather than the underlying substrate. To address this issue and maintain selectivity over a high number of ALD cycles, a second approach has been used: incorporating a cyclic etching step into the ALD cycles. Hashemi et al. demonstrated the removal of ODPA SAMs after using them for selective deposition of Al_2O_3 on Cu surfaces.⁷⁶ Although the combined process of deposition and etching was solution-based and the etching was performed ex-situ, the authors showed that unwanted deposits could be removed along with the SAM, thereby enhancing overall selectivity. In another paper on the reapplication of Hacac as an inhibitor to enhance the selectivity of SiO_2 , as discussed above, the same group of Mackus and co-workers showed that an additional step of exposing the substrate to H_2 plasma results in etch and removal of the inhibitor species, leaving a clean NGS for inhibitor adsorption in the next ALD cycle.⁷⁷ Other groups have also shown the benefit of cyclical etching in AS-ALD.^{78,79}

Maintaining high selectivity through effective correction steps for inhibitors is crucial for ensuring the precision and efficiency of AS-ALD processes. The proper application of these correction steps can significantly improve the outcome, particularly in complex material systems where high fidelity and minimal defect deposition are essential.

3. ALD PRECURSORS

3.1. Introduction to Precursors in the ALD Process.

The ALD precursor is arguably the most important component of an ALD process. The precursor comprises a metal center and surrounding ligands, and its suitability for the process hinges on several criteria. These include possessing a vapor pressure adequate for delivery into the chamber, maintaining thermal stability to avoid decomposition at the ALD process temperature, and exhibiting reactivity conducive to depositing the desired film and—for AS-ALD—conducive to selective surface adsorption and reaction.⁸⁰

Precursor reactivity, crucial for effective surface interaction, can vary depending on the ligand type. Common precursor ligands include alkyl, alkylamido, alkoxyde, and halide types, as shown in Figure 8, each with distinct characteristics. Alkyl ligands, attractive for their simplicity and high reactivity, are widely employed. For instance, trimethylaluminum is a well-known alkyl-containing precursor due to its high volatility and strong reactivity with water, leading to efficient ALD of Al_2O_3 films. However, the high reactivity can also pose challenges, such as unwanted side reactions.¹¹ As will be discussed later, this can be a factor in reducing selectivity in the AS-ALD process. Alkylamido ligands offer heightened reactivity but can suffer from poor thermal stability. For example, tetrakis-(dimethylamido)titanium (TDMATi) is commonly used to

deposit TiN films. Despite its reactivity, the thermal decomposition can lead to carbon and nitrogen contamination and nonuniform film growth.⁸¹ Alkoxyde ligands provide improved thermal stability but are susceptible to phenomena such as beta-hydride elimination. For example, titanium isopropoxide (TTIP) is a well-known alkoxyde precursor for TiO_2 deposition, and its stability allows for high-temperature ALD processes, which are beneficial for applications requiring robust films.⁸² However, beta-hydride elimination within the alkoxyde ligand can generate byproducts such as H_2O vapor, alcohols, or surface hydroxyl groups during ligand decomposition. These byproducts can also initiate secondary chain reactions with remaining alkoxyde ligands, disrupting the self-limiting surface reaction characteristic of ALD and leading to nonideal growth behavior. To mitigate these undesired effects, careful process control is required, including the optimization of deposition parameters, such as reducing the process temperature.⁸³ Meanwhile, while advantageous for minimizing carbon impurities, halide ligands may compromise electrical properties due to their potential to introduce unwanted halogen impurities. For example, HfCl_4 is a widely used halide precursor for HfO_2 ALD. While HfCl_4 enables low-carbon films, residual chlorine can degrade electrical properties.⁸⁴

Given the different behaviors of the various ALD precursors, selecting an appropriate precursor requires careful consideration of factors such as thermal decomposition temperature and intended application to ensure optimal process performance and material characteristics. Toward a better understanding of precursor selection, some studies have explored the effect of varying a precursor's ligand type for a given metal center and substrate, with a focus on the ALD growth characteristics, the chemical or physical properties of the resulting thin film, or the electrical performance of devices fabricated with the films. Although numerous studies have explored the comparative effects of precursor ligand types, particularly their size, reactivity, and polarity, on ALD growth characteristics,^{80,84–89} here we illustrate just a few examples.

The Ru ALD process has been extensively studied to understand the influence of precursor ligand tuning on growth characteristics, particularly in minimizing nucleation delays.⁸⁵ Notably, variations in ligand structure, even at the same Ru oxidation state, significantly impact nucleation behavior. For example, precursors such as $\text{Ru}(\text{EtCp})_2$ and $\text{Ru}(\text{Cp})_2$ exhibit nucleation delays exceeding 200 cycles, whereas other precursors, such as (ethylcyclopentadienyl)(pyrrolyl)-ruthenium (ECPR) and bis(2,5-dimethylpyrrolyl)ruthenium (DMPR), demonstrate significantly reduced nucleation delays ranging from 25 to 60 cycles.⁸⁵ This ligand-dependent effect on growth characteristics can also be observed in terms of surface coverage and ALD temperature window across other

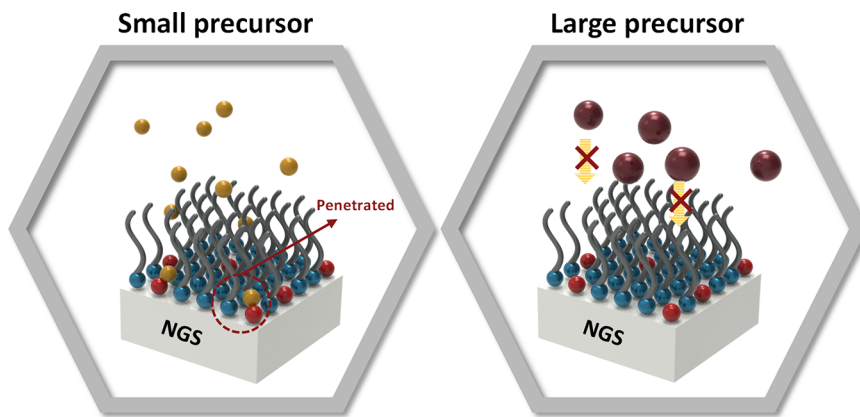


Figure 9. Schematic of the effect of precursor size in the AS-ALD process. In the left image, smaller precursors can potentially penetrate the gaps between inhibitors, allowing them to react with exposed reactive sites on the substrate surface. Conversely, in the right image, larger precursors are less likely to infiltrate these gaps, resulting in more effective blocking by the inhibitors.

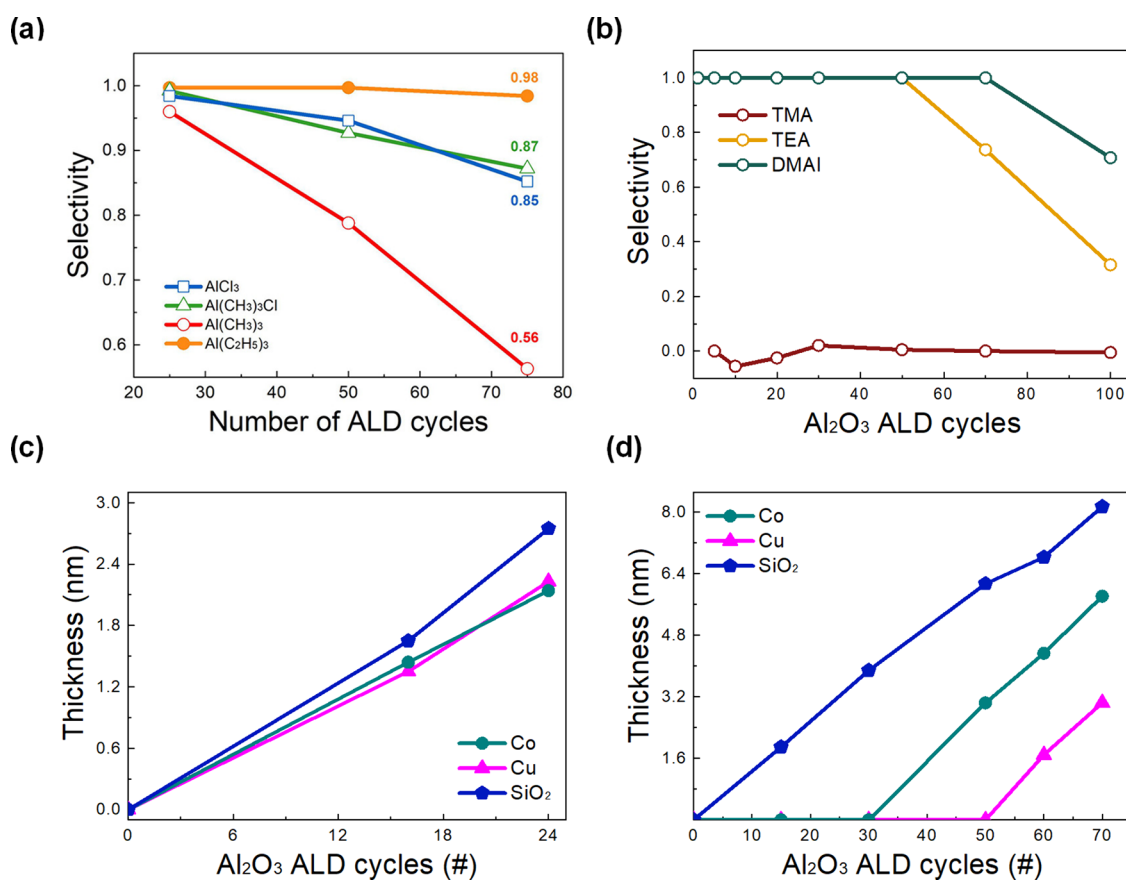


Figure 10. Three different Al₂O₃ AS-ALD systems demonstrating the importance of precursor selection on selectivity. (a) The selectivity of Al₂O₃ ALD on SiO₂/Si compared to that on SAM-covered SiO₂/Si as a function of the number of ALD cycles for various Al precursors. Reproduced from ref 27. Copyright 2021 American Chemical Society. (b) The selectivity of Al₂O₃ ALD on Cu compared to that on nitropropane-inhibited Cu as a function of the number of ALD cycles for three different Al precursors. Reproduced from ref 92. Copyright 2023 American Chemical Society. (c,d) The thickness of ALD Al₂O₃ on the ethanethiol-inhibited substrates as a function of the number of ALD cycles using (c) TMA and (d) DMAI. Reproduced from ref 91. Copyright 2020 American Chemical Society.

ALD systems, highlighting the critical role of ligand design in ALD processes. Lee et al. conducted Pt ALD at low temperatures utilizing either MeCpPtMe₃ or hexadiene dimethyl platinum (HDMP) and showed that HDMP exhibited a low activation energy for surface reactions, facilitating higher coverage within shorter ALD cycles than MeCpPtMe₃.⁸⁶

Furthermore, Oh et al. showed that the number of Cl atoms in the Al precursor significantly influences the ALD temperature window. Specifically, increasing the number of Cl atoms in the Al(CH₃)_xCl_{3-x} precursor increases the activation barrier for adsorption, thereby narrowing the ALD process window at lower temperatures.⁸⁹ Moreover, changes in ligand structure affect nucleation behavior and surface interactions, ultimately shaping the microstructure and electrical performance of the

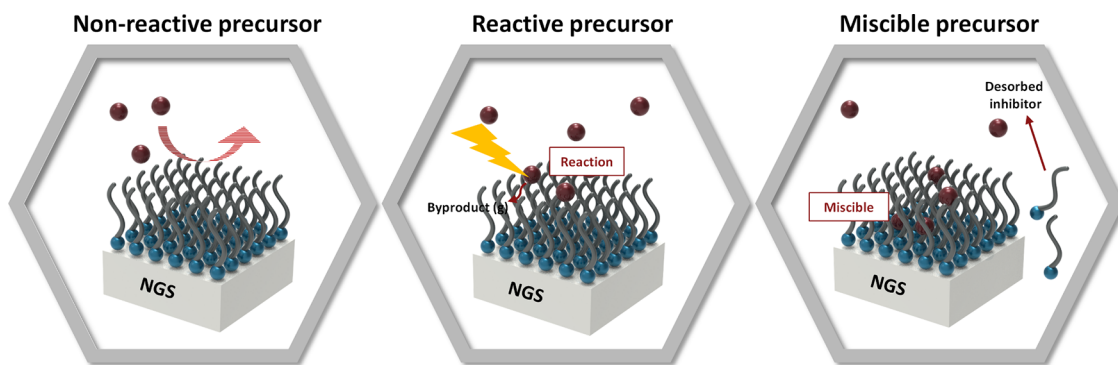


Figure 11. Schematic illustration of precursor properties that may drive exceptions to the frequent observation that larger precursors are easier to inhibit than smaller precursors in AS-ALD. The standard case is shown on the left for a nonreactive precursor. Exceptions include direct reactivity between the ALD precursor and the inhibitor (middle) and the miscibility of the ALD precursor within the inhibitor layer (right).

deposited films. For instance, in a comparative analysis of HfCl_4 and $\text{Hf}(\text{EtCp})_2\text{Cl}_2$, the substitution of two Cl atoms in HfCl_4 with EtCp ligands yielded smoother thin films and markedly reduced leakage current density in metal oxide semiconductor (MOS) capacitors, attributed to diminished Cl impurities within the thin film. The HfO_2 film grown with $\text{Hf}(\text{EtCp})_2\text{Cl}_2$ exhibited superior electrical properties, including reduced leakage current density.⁸⁴

3.2. Effect of Precursor Size on Selectivity. Compared to the literature on ALD precursor selection, comparative investigations of precursors in AS-ALD have been much less researched. To support this research direction, Kim et al. recently reviewed the requirements and challenges for the molecular properties of the AS-ALD precursors.⁹⁰ It is important to note that the optimal criteria for AS-ALD precursor selection may differ significantly from the selection criteria for simple ALD. For example, whereas precursors with high reactivity may be desirable to achieve good nucleation and growth in ALD, overly facile reactivity may make those same precursors unsuitable for AS-ALD if their reaction chemistry is too hard to inhibit. Nevertheless, the characteristics of an ALD precursor that vary depending on the ligand type, such as the size, structure, and reactivity, can also be tuned—albeit in different ways—to affect selectivity in AS-ALD.

Among these factors, the size of the ALD precursor has been the most frequently reported. Inhibitors such as SAMs and SMIs typically attach to the surface by adsorbing onto discrete reactive sites on the NGS. Empty spaces may exist between inhibitor molecules depending on the distribution of those reactive surface sites and the steric hindrance of the inhibitor molecules. Therefore, according to a simple conceptual picture as shown in Figure 9, if an ALD precursor is small enough, it may penetrate these gaps and initiate thin film formation. This can occur either through physical adsorption within the inhibitor layer or by binding to reactive sites left exposed on the substrate due to incomplete inhibitor coverage. In this process, additional surface groups, such as siloxane groups on SiO_2 , could also act as potential adsorption sites. While these groups are less reactive than hydroxyl groups, they can still contribute to initial nucleation. Physisorption of precursor may also occur, compounding the loss of selectivity. However, larger precursors may have difficulty passing through the space between the inhibitors, preventing them from either absorbing into the inhibitor layer or reaching the underlying substrate and adsorbing at its surface. Thus, the inhibitor acts like a sieve, filtering out larger precursor molecules and making it

more difficult for the precursor to adsorb on reactive sites and initiate film deposition.

In general, the adsorption of precursor molecules into the gaps between inhibitor molecules will cause the inhibitor to lose its blocking ability, reducing selectivity. Consequently, quite a few studies have reported that higher selectivity was obtained using larger ALD precursors when comparing several ALD precursors with the same inhibitor for both SAM and SMI inhibitors.^{22,27,28,50,91,92} Most of the literature studies to date have focused on a comparison of aluminum precursors. Our group has reported Al precursor comparisons across several different inhibitor systems in AS-ALD. In one series, shown in Figure 10(a), we performed AS-ALD of Al_2O_3 using TMA, triethylaluminum (TEA), aluminum chloride (AlCl_3), or dimethylaluminum chloride ($\text{Al}(\text{CH}_3)_2\text{Cl}$) on a SiO_2 substrate inhibited with an OTDS SAM. The effective sizes of these precursors, after taking into account their propensity to dimerize, are 87.2, 140.2, 143.7, and 151.6 Å³, respectively. Results showed that TMA exhibited the lowest selectivity; this effect was attributed to TMA having the smallest effective average size of the precursor series, allowing it to penetrate between the OTDS molecules.²⁷

Another study compared the selectivity of AS-ALD using dimethylaluminum isopropoxide (DMAI) and TMA precursors on a Cu substrate treated with an MSA SMI. The results showed that DMAI exhibited higher selectivity than TMA. This higher selectivity was attributed to the tendency of DMAI to exist as a dimer, making its effective size much larger than that of TMA.^{28,93} Our group also conducted a comparative study of selectivity using TMA, TEA, and DMAI on a Cu substrate treated with a nitropropane SMI. The results again indicated that TMA had the lowest selectivity, followed by TEA, with DMAI exhibiting the highest selectivity across the most ALD cycles, as shown in Figure 10(b). This trend is consistent with the precursor size order, supporting the idea that precursor size influences selectivity.⁹² Yet another SMI study yielded similar conclusions: when comparing the selectivity of TMA and TEA on a SiO_2 substrate blocked with a TMPS inhibitor, TEA demonstrated higher selectivity than TMA.²²

The effect of precursor size on selectivity has been reported fairly consistently across multiple research groups. Kim et al. performed ALD using TMA and DMAI on Co and Cu substrates with an ethanethiol inhibitor, achieving better blocking with the larger-sized DMAI, as shown in Figures 10(c) and (d). Merkx et al. examined ALD precursor

adsorption at the substrate using TMA, DMAI, and tris(dimethylamino) aluminum (TDMAA) on surfaces inhibited by Hacac.⁹⁴ Their results showed that TMA was adsorbed to the NGS, suggesting it may exhibit the lowest selectivity because of its small size. In summary, by comparing various reports, the primary trend indicates that precursor size significantly affects selectivity, with higher selectivity obtained from larger-sized precursors. This trend underscores the importance of considering ALD precursor dimensions when designing AS-ALD processes.

3.3. When Precursor Size Is Not the Dominant Property in Selectivity. Despite the strong evidence for the beneficial effect that larger precursors provide in achieving selectivity in AS-ALD, results that deviate from this trend have also been reported. In particular, low selectivity may still be observed even when large ALD precursors are used. Based on the literature, we categorize the origin of these exceptions to the “bigger is better” rule into three phenomena: (1) reaction between precursor and inhibitor, (2) miscibility of the precursor into the inhibitor layer, and (3) impact of the central metal atom. The first two effects are illustrated schematically in Figure 11.

In case (1), even if the precursor is large, if it reacts with the inhibitor, then the inhibitor may lose its inherent blocking properties. This, in turn, could enable the subsequent adsorption of precursors and counter-reactants and the eventual formation of a thin film. In one recent example from our group,²⁶ an investigation of three different Hf precursors on the same inhibition layer showed selectivities that did not correlate with precursor size but instead were attributed to the existence of a direct reaction pathway between a precursor and the inhibitor. In that study, a SiO₂ surface was treated with DIPAS, which produced SiH₃-termination. The SiH₃-terminated surface subsequently showed good blocking ability for HfO₂ ALD using Hf(O^tBu)₄ and HfCl₄ precursors but elicited no selectivity for TDMAHf, as shown in Figure 12(a). To investigate this effect in detail, we used DFT calculations to examine the reaction mechanism between TDMAHf and SiH₃. The results revealed that TDMAHf, with the methyl methylene imine (MMI) ligand formed by an intramolecular reaction within TDMAHf, has an energetically favorable pathway with surface SiH₃ species (Figure 12(b)). This side reaction between the precursor and the inhibitor was hypothesized to lead to low selectivity.²⁶

Such decreased selectivity due to the reaction between the precursor and inhibitor has also been reported in other studies. Delabie and co-workers performed TiO₂ AS-ALD using TiCl₄ and Ti(OCH₃)₄ on a DMATMS-treated SiO₂ surface.⁹⁵ According to the results in Figure 12(c), the larger Ti(OCH₃)₄ showed lower selectivity than TiCl₄, providing another exception to the “bigger is better” rule. After pulsing each precursor, they observed changes in the water contact angle (WCA) of the DMATMS-treated surface and confirmed that WCA decreased after pulsing Ti(OCH₃)₄ in the ALD sequence. This observation indicated that the precursor adsorbed on Si(CH₃)₃, altering the surface properties and resulting in a loss of blocking ability against subsequent precursor exposure.⁹⁵

In addition to case (1), in which the blocking ability is lost due to the reaction of the ALD precursor with the inhibitor, precursor miscibility within the inhibitor can also affect selectivity (case (2)). The effect is illustrated schematically in Figure 11. We recently confirmed that three Al precursors

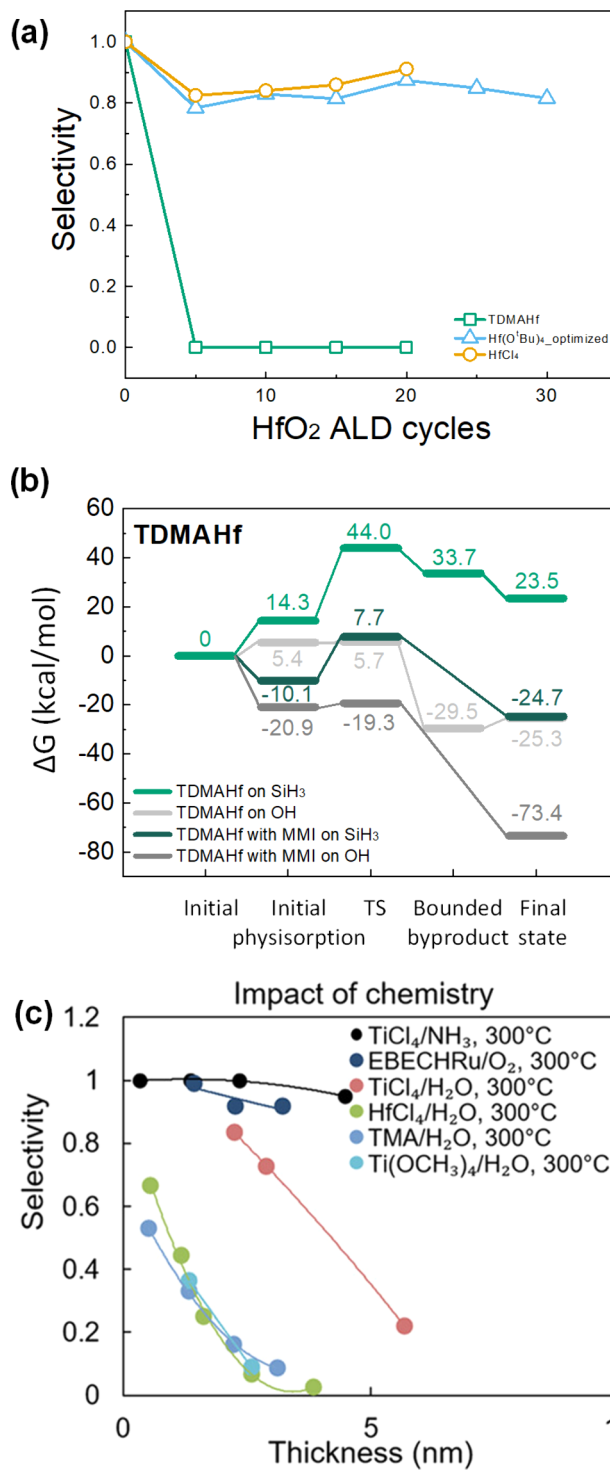


Figure 12. (a) Selectivity of HfO₂ ALD on DIPAS-treated TiN compared to DIPAS-treated SiO₂ as a function of the number of ALD cycles for three different Hf precursors. (b) Free energy diagrams calculated by DFT for adsorption of TDMAHf. Panels a and b are reproduced from ref 26. Copyright 2024 American Chemical Society. (c) Selectivity versus thickness for varying deposition chemistries using DMATMS as an inhibitor. Panel c reproduced from ref 95. Copyright 2020 American Chemical Society.

showed different behaviors on a Cu substrate treated with benzenethiol (BT) but that the differences do not correlate in the expected way with precursor size. Benzenethiol exists as a semicrystalline multilayer on Cu. Upon this inhibitor film,

DMAI showed excellent selectivity in Al_2O_3 ALD, but both TMA and TEA exhibited no selectivity, nucleating on BT immediately. Moreover, changes in the thickness of the BT multilayer occurred when pulsing each precursor, with TEA degrading the inhibitor layer faster than TMA. We hypothesize that TEA may be more miscible within the benzenethiol layer due to its longer ethyl ligands. These results suggest that precursor ligand miscibility, rather than precursor size alone, plays a role in the benzenethiol layer.

The metal center of the ALD precursor can also affect selectivity (case (3)). One exemplary case is the AS-ALD of TEA and DEZ on the same BT-treated Cu substrate. Despite having the same ethyl ligand, DEZ showed excellent selectivity, unlike TEA, which did not show selectivity. We speculate that differences in Lewis acidity due to the different metal centers may determine the interaction between the precursor and inhibition layer beyond the ligand type. A similar trend has been reported in other studies. In two separate studies of AS-ALD on ODTs-treated SiO_2 substrates using TEA²⁷ and DEZ,³⁶ DEZ showed slightly better selectivity than TMA. Comparing the thicknesses that can be selectively deposited, ZnO maintained more than 95% selectivity up to 8.5 nm, whereas Al_2O_3 could maintain 95% selectivity only up to 6 nm. Notably, the effect is much smaller than in the BT case. The difference may be due to different growth temperatures used in the two ODTs-based processes, or it may be that the reactivity between the metal center and the ODTs SAM is different from that between the metal center and the BT multilayer.

Other comparisons are also instructive in demonstrating the effect of the metal center with similar ligands. As shown in Figure 12(c), Soethoudt et al. compared HfCl_4 and TiCl_4 on DMATMS-treated SiO_2 substrate. Despite its larger size, HfCl_4 showed lower selectivity compared to TiCl_4 .⁹⁵ The authors observed a WCA change after precursor pulsing and noted that unlike TiCl_4 , which showed no change in WCA, the WCA decreased for HfCl_4 , suggesting that HfCl_4 adsorbed onto the $\text{Si}(\text{CH}_3)_3$ on the surface. Although their alkyl ligands are not the same, a comparison of TMA and DEZ can also be insightful because their van der Waals volumes are similar (84.4 \AA^3 and 93.3 \AA^3 , respectively). Our group has compared the selectivity of TMA and DEZ on DDT-treated substrates. The results showed that DEZ had a higher selectivity than TMA, which could be attributed to its lower Lewis acidity.⁹⁶ Similar results are also found when comparing the work across research groups: a study by Mori et al.⁹⁷ using DEZ on DDT-treated Cu substrates showed better selectivity than that with TMA on DDT-treated Cu by Liu et al.⁹⁶

Considering previous reports, while the general observation has been that larger precursors lead to better blocking and higher selectivity, several exceptions to this “rule” have also been reported. Our organized analysis highlights that the chemical interactions between inhibitors and precursors are crucial in determining selectivity. Specifically, the reactivity between the precursor and inhibitor can compromise the inhibitor’s blocking ability, thereby diminishing selectivity. Also, the miscibility of the precursor within the inhibitor layer may similarly lead to a loss of selectivity. Moreover, even with identical ligands, differences in the metal center can alter Lewis acidity, further influencing selectivity. Therefore, understanding the interplay of these factors can lead to more informed decisions in precursor selection and the development of more effective inhibition strategies.

4. CONCLUSIONS AND OUTLOOK

The need for innovative fabrication approaches in modern electronic devices, driven by demands for higher speed, lower power consumption, and lower costs, together with increased integration and rapid processing time, has underscored the limitations of conventional top-down patterning techniques such as photolithography. Consequently, there has been a growing focus on bottom-up patterning methods, particularly AS-ALD, which offer precise control over nanostructure fabrication and potential defect mitigation. AS-ALD has shown promise in depositing materials exclusively in targeted regions, thus simplifying fabrication processes by reducing lithography requirements and minimizing process steps and costs. It is also highly suitable for advanced 3D integrated devices, highlighting its essential role in advancing semiconductor technology.

AS-ALD can be implemented through activation, deactivation, and inherent methods, with deactivation (using SAMs, SMIs, and polymers) being the most common approach due to its ability to block unwanted precursor adsorption and enhance thin film selectivity. Achieving effective selectivity requires understanding the chemical interactions between inhibitors, substrates, and ALD precursors. While larger precursors generally yield higher selectivity by limiting penetration, this review highlights other factors, including direct precursor-inhibitor reactions, miscibility with the inhibition layer, and variations in metal centers and Lewis acidities. Selecting appropriate ALD precursors is, therefore, essential for optimizing AS-ALD processes. Similarly, choosing effective SAMs and SMIs is critical. SAMs form densely packed monolayers, while SMIs rely on smaller chemisorptive groups. Both use acid–base interactions between head groups and substrates to enhance selectivity, while inert tail groups act as barriers to deposition. The number and reactivity of lone pairs on termination groups of the inhibitor also play a key role in precursor interaction and selectivity.

Future research in AS-ALD should prioritize the development of new inhibitors with tailored properties that enhance selectivity, thermal stability, and compatibility with advanced semiconductor processes. Designing inhibitors capable of operating effectively under extreme conditions, such as high temperatures or within highly reactive environments, will be particularly important as semiconductor technology scales down to smaller nodes. Moreover, exploring novel formulations of SAMs and SMIs, including those incorporating aromatic and fluorocarbon backbones, may yield inhibitors with improved chemical stability, greater coverage uniformity, and higher resistance to unwanted precursor adsorption. These advancements could unlock new possibilities for achieving selective deposition on increasingly complex substrate geometries.

In addition to advancing inhibitor design, future efforts should emphasize a holistic approach to selectivity that considers the interplay between inhibitors, ALD precursors, and substrate surfaces. While current studies often examine these factors in isolation, high selectivity demands a deeper understanding of how these components interact in real-world conditions. For instance, the chemical compatibility between inhibitors and precursors, the miscibility of inhibition layers with precursors, and the specific interactions of metal centers and ligands with various surfaces must all be carefully optimized for each material system. Collaborative research

combining experimental techniques and advanced computational modeling could offer important insights into these interactions, facilitating the rational design of AS-ALD processes. Another promising direction is the integration of AS-ALD with other cutting-edge fabrication techniques, such as area-selective etching (ASE), 3D nanoarchitectures, and atomic precision manufacturing. This integration could address some of the current limitations in AS-ALD, such as selectivity on high-aspect-ratio structures, and enable unprecedented control over thin film deposition at the atomic scale. Additionally, hybrid approaches that combine AS-ALD with self-assembly or machine learning-driven optimization could accelerate the discovery of optimal material combinations and processing conditions.

As the field progresses, AS-ALD plays a critical role in the fabrication of next-generation electronic devices, including advanced transistors, memory devices, and quantum computing components. Its ability to selectively deposit precise thin films will be essential for addressing the high-performance and reliability demands of future technologies. Continuous advancements in AS-ALD will enhance device performance and contribute to the development of more energy-efficient and sustainable manufacturing processes, aligning with global efforts to reduce the environmental footprint of semiconductor production.

■ AUTHOR INFORMATION

Corresponding Author

Stacey F. Bent — Department of Chemical Engineering, Stanford University, Stanford, California 94305, United States; Department of Energy Science and Engineering, Stanford University, Stanford, California 94305, United States;  orcid.org/0000-0002-1084-5336; Email: sbent@stanford.edu

Authors

Yujin Lee — Department of Chemical Engineering, Stanford University, Stanford, California 94305, United States;  orcid.org/0000-0002-9213-019X

Amnon Rothman — Department of Chemical Engineering, Stanford University, Stanford, California 94305, United States;  orcid.org/0000-0002-7095-8279

Alexander B. Shearer — Department of Chemical Engineering, Stanford University, Stanford, California 94305, United States;  orcid.org/0000-0002-4128-2636

Complete contact information is available at:

<https://pubs.acs.org/10.1021/acs.chemmater.4c02902>

Author Contributions

§Y.L. and A.R. are co-first authors.

Notes

The authors declare no competing financial interest.

■ ACKNOWLEDGMENTS

This work was supported by the U.S. Department of Energy under award number DE-SC0004782 (A.R. and S.F.B.). This work was also supported as part of the Center for High Precision Patterning Science (CHiPPS), an Energy Frontier Research Center funded by the U.S. Department of Energy, Office of Science, Basic Energy Sciences (Y.L.). Part of this work was performed at the Stanford Nano Shared Facilities

(SNSF), supported by the National Science Foundation under award number ECCS-2026822.

■ REFERENCES

- Clark, R.; Tapily, K.; Yu, K. H.; Hakamata, T.; Consiglio, S.; O'Meara, D.; Wajda, C.; Smith, J.; Leusink, G. Perspective: New process technologies required for future devices and scaling. *APL Materials* **2018**, *6* (5), 58203.
- Parsons, G. N.; Clark, R. D. Area-Selective Deposition: Fundamentals, Applications, and Future Outlook. *Chem. Mater.* **2020**, *32* (12), 4920–4953.
- Carlsson, J. O. Novel and selective vapor deposition processes. *Vacuum* **1990**, *41* (4), 1077–1080.
- Hampden-Smith, M. J.; Kodas, T. T. Chemical vapor deposition of metals: Part 2. Overview of selective CVD of Metals. *Chem. Vap. Deposition* **1995**, *1* (2), 39–48.
- Carlsson, J.-O. Selective vapor-phase deposition on patterned substrates. *Critical Reviews in Solid State and Materials Sciences* **1990**, *16* (3), 161–212.
- Jiang, X.; Bent, S. F. Area-Selective ALD with Soft Lithographic Methods: Using Self-Assembled Monolayers to Direct Film Deposition. *J. Phys. Chem. C* **2009**, *113* (41), 17613–17625.
- Mackus, A. J. M.; Bol, A. A.; Kessels, W. M. M. The use of atomic layer deposition in advanced nanopatterning. *Nanoscale* **2014**, *6* (19), 10941–10960.
- Mackus, A. J. M.; Merkx, M. J. M.; Kessels, W. M. M. From the Bottom-Up: Toward Area-Selective Atomic Layer Deposition with High Selectivity. *Chem. Mater.* **2019**, *31* (1), 2–12.
- Parsons, G. N. Functional model for analysis of ALD nucleation and quantification of area-selective deposition. *Journal of Vacuum Science & Technology A* **2019**, *37* (2), 020911.
- Cao, K.; Cai, J.; Chen, R. Inherently Selective Atomic Layer Deposition and Applications. *Chem. Mater.* **2020**, *32* (6), 2195–2207.
- George, S. M. Atomic Layer Deposition: An Overview. *Chem. Rev.* **2010**, *110* (1), 111–131.
- Kim, W. H.; Minaye Hashemi, F. S.; Mackus, A. J. M.; Singh, J.; Kim, Y.; Bobb-Semple, D.; Fan, Y.; Kaufman-Osborn, T.; Godet, L.; Bent, S. F. A Process for Topographically Selective Deposition on 3D Nanostructures by Ion Implantation. *ACS Nano* **2016**, *10* (4), 4451–4458.
- Yarbrough, J.; Shearer, A. B.; Bent, S. F. Next generation nanopatterning using small molecule inhibitors for area-selective atomic layer deposition. *Journal of Vacuum Science & Technology A* **2021**, *39* (2), 21002.
- Zheng, L.; He, W.; Spampinato, V.; Franquet, A.; Sergeant, S.; Gendt, S. D.; Armini, S. Area-Selective Atomic Layer Deposition of TiN Using Trimethoxy(octadecyl)silane as a Passivation Layer. *Langmuir* **2020**, *36* (44), 13144–13154.
- Seo, S.; Yeo, B. C.; Han, S. S.; Yoon, C. M.; Yang, J. Y.; Yoon, J.; Yoo, C.; Kim, H. J.; Lee, Y. B.; Lee, S. J.; Myoung, J. M.; Lee, H. B. R.; Kim, W. H.; Oh, I. K.; Kim, H. Reaction Mechanism of Area-Selective Atomic Layer Deposition for Al_2O_3 Nanopatterns. *ACS Appl. Mater. Interfaces* **2017**, *9* (47), 41607–41617.
- Chang, C. W.; Hsu, H. H.; Hsu, C. S.; Chen, J. T. Achieving area-selective atomic layer deposition with fluorinated self-assembled monolayers. *Journal of Materials Chemistry C* **2021**, *9* (41), 14589–14595.
- de Paula, C.; Bobb-Semple, D.; Bent, S. F. Increased selectivity in area-selective ALD by combining nucleation enhancement and SAM-based inhibition. *J. Mater. Res.* **2021**, *36* (3), 582–591.
- Hong, J.; Porter, D. W.; Sreenivasan, R.; McIntyre, P. C.; Bent, S. F. ALD resist formed by vapor-deposited self-assembled monolayers. *Langmuir* **2007**, *23* (3), 1160–1165.
- Lee, H.-B.-R.; Kim, H. Area Selective Atomic Layer Deposition of Cobalt Thin Films. *ECS Trans.* **2008**, *16* (4), 219–225.
- Niinistö, J.; Putkonen, M.; Niinistö, L.; Stoll, S. L.; Kukli, K.; Sajavaara, T.; Ritala, M.; Leskelä, M. Controlled growth of HfO_2 thin films by atomic layer deposition from cyclopentadienyl-type precursor and water. *J. Mater. Chem.* **2005**, *15* (23), 2271–2275.

- (21) Khan, R.; Shong, B.; Ko, B. G.; Lee, J. K.; Lee, H.; Park, J. Y.; Oh, I. K.; Raya, S. S.; Hong, H. M.; Chung, K. B.; Luber, E. J.; Kim, Y. S.; Lee, C. H.; Kim, W. H.; Lee, H. B. R. Area-Selective Atomic Layer Deposition Using Si Precursors as Inhibitors. *Chem. Mater.* **2018**, *30* (21), 7603–7610.
- (22) Yarbrough, J.; Pieck, F.; Grigjanis, D.; Oh, I.-K.; Maue, P.; Tonner-Zech, R.; Bent, S. F. Tuning Molecular Inhibitors and Aluminum Precursors for the Area-Selective Atomic Layer Deposition of Al_2O_3 . *Chem. Mater.* **2022**, *34* (10), 4646–4659.
- (23) Jaeger, R. C. *Introduction to Microelectronic Fabrication*; Addison-Wesley Publishing Company, 1988.
- (24) Taur, Y.; Ning, T. H. *Fundamentals of Modern VLSI Devices*; Cambridge University Press, 2013.
- (25) Zhang, Y.; Discekici, E. H.; Burns, R. L.; Somervell, M. H.; Hawker, C. J.; Bates, C. M. Single-Step, Spin-on Process for High Fidelity and Selective Deposition. *ACS Applied Polymer Materials* **2020**, *2* (2), 481–486.
- (26) Lee, Y.; Seo, S.; Shearer, A. B.; Werbrouck, A.; Kim, H.; Bent, S. F. HfO_2 Area-Selective Atomic Layer Deposition with a Carbon-Free Inhibition Layer. *Chem. Mater.* **2024**, *36* (9), 4303–4314.
- (27) Oh, I.-K.; Sandoval, T. E.; Liu, T.-L.; Richey, N. E.; Bent, S. F. Role of Precursor Choice on Area-Selective Atomic Layer Deposition. *Chem. Mater.* **2021**, *33* (11), 3926–3935.
- (28) Yarbrough, J.; Pieck, F.; Shearer, A. B.; Maue, P.; Tonner-Zech, R.; Bent, S. F. Area-Selective Atomic Layer Deposition of Al_2O_3 with a Methanesulfonic Acid Inhibitor. *Chem. Mater.* **2023**, *35* (15), 5963–5974.
- (29) Liu, Y. Self-assembled Monolayers. In *Encyclopedia of Tribology*; Wang, Q. J., Chung, Y.-W., Eds.; Springer US, 2013; pp 2997–3001.
- (30) Pasquali, M.; De Gendt, S.; Armini, S. Understanding the impact of Cu surface pre-treatment on Octadecanethiol-derived self-assembled monolayer as a mask for area-selective deposition. *Appl. Surf. Sci.* **2021**, *540*, 148307.
- (31) Bergsman, D. S.; Liu, T.-L.; Closser, R. G.; Nardi, K. L.; Draeger, N.; Hausmann, D. M.; Bent, S. F. Formation and Ripening of Self-Assembled Multilayers from the Vapor-Phase Deposition of Dodecanethiol on Copper Oxide. *Chem. Mater.* **2018**, *30* (16), 5694–5703.
- (32) Chang, C. W.; Tseng, Y. H.; Hsu, C. S.; Chen, J. T. Area-Selective Atomic Layer Deposition on Metal/Dielectric Patterns: Amphiphobic Coating, Vaporizable Inhibitors, and Regenerative Processing. *ACS Appl. Mater. Interfaces* **2023**, *15* (23), 28817–28824.
- (33) Clerix, J. J.; Sanz-Matias, A.; Armini, S.; Harvey, J. N.; Delabie, A. Structural Phases of Alkanethiolate Self-Assembled Monolayers (C_{1-12}) on Cu[100] by Density Functional Theory. *J. Phys. Chem. C* **2020**, *124* (6), 3802–3811.
- (34) Lee, J.; Lee, J. M.; Ahn, J. H.; Park, T. J.; Kim, W. H. Area-Selective Atomic Layer Deposition Using Vapor Dosing of Short-Chain Alkanethiol Inhibitors on Metal/Dielectric Surfaces. *Advanced Materials Interfaces* **2022**, *9* (13), 2102364.
- (35) Liu, T.-L.; Nardi, K. L.; Draeger, N.; Hausmann, D. M.; Bent, S. F. Effect of Multilayer versus Monolayer Dodecanethiol on Selectivity and Pattern Integrity in Area-Selective Atomic Layer Deposition. *ACS Appl. Mater. Interfaces* **2020**, *12* (37), 42226–42235.
- (36) Liu, T. L.; Zeng, L.; Nardi, K. L.; Hausmann, D. M.; Bent, S. F. Characterizing Self-Assembled Monolayer Breakdown in Area-Selective Atomic Layer Deposition. *Langmuir* **2021**, *37* (39), 11637–11645.
- (37) Minaye Hashemi, F. S.; Birchansky, B. R.; Bent, S. F. Selective Deposition of Dielectrics: Limits and Advantages of Alkanethiol Blocking Agents on Metal-Dielectric Patterns. *ACS Appl. Mater. Interfaces* **2016**, *8* (48), 33264–33272.
- (38) Zoha, S.; Pieck, F.; Gu, B.; Tonner-Zech, R.; Lee, H.-B.-R. Organosulfide Inhibitor Instigated Passivation of Multiple Substrates for Area-Selective Atomic Layer Deposition of HfO_2 . *Chem. Mater.* **2024**, *36* (6), 2661–2673.
- (39) Bobb-Semple, D.; Zeng, L.; Cordova, I.; Bergsman, D. S.; Nordlund, D.; Bent, S. F. Substrate-Dependent Study of Chain Orientation and Order in Alkylphosphonic Acid Self-Assembled Monolayers for ALD Blocking. *Langmuir* **2020**, *36* (43), 12849–12857.
- (40) Fickenscher, G.; Steffen, J.; Görling, A.; Libuda, J. Atomic Layer Deposition of HfS_2 on Functionalized Self-Assembled Monolayers on Ordered Oxide Surfaces: A Model Study under UHV Conditions. *J. Phys. Chem. C* **2024**, *128* (2), 798–809.
- (41) Jeong, N. C.; Lee, J. S.; Tae, E. L.; Lee, Y. J.; Yoon, K. B. Acidity Scale for Metal Oxides and Sanderson's Electronegativities of Lanthanide Elements. *Angew. Chem., Int. Ed.* **2008**, *47* (52), 10128–10132.
- (42) Karasulu, B.; Roozeboom, F.; Mameli, A. High-Throughput Area-Selective Spatial Atomic Layer Deposition of SiO_2 with Interleaved Small Molecule Inhibitors and Integrated Back-Etch Correction for Low Defectivity. *Adv. Mater.* **2023**, *35* (25), 2301204.
- (43) Klement, P.; Anders, D.; Gümbel, L.; Bastianello, M.; Michel, F.; Schörmann, J.; Elm, M. T.; Heiliger, C.; Chatterjee, S. Surface Diffusion Control Enables Tailored-Aspect-Ratio Nanostructures in Area-Selective Atomic Layer Deposition. *ACS Appl. Mater. Interfaces* **2021**, *13* (16), 19398–19405.
- (44) Li, J.; Tezsevin, I.; Merkx, M. J. M.; Maas, J. F. W.; Kessels, W. M. M.; Sandoval, T. E.; Mackus, A. J. M. Packing of inhibitor molecules during area-selective atomic layer deposition studied using random sequential adsorption simulations. *Journal of Vacuum Science & Technology A* **2022**, *40* (6), 062409–1.
- (45) Liu, T.-L.; Bent, S. F. Area-Selective Atomic Layer Deposition on Chemically Similar Materials: Achieving Selectivity on Oxide/Oxide Patterns. *Chem. Mater.* **2021**, *33* (2), 513–523.
- (46) Satyarthi, S.; Hasan Ul Iqbal, M.; Abida, F.; Nahar, R.; Hauser, A. J.; Cheng, M. M.-C.; Ghosh, A. Stearic Acid as an Atomic Layer Deposition Inhibitor: Spectroscopic Insights from AFM-IR. *Nanomaterials* **2023**, *13* (19), 2713.
- (47) Mameli, A.; Merkx, M. J. M.; Karasulu, B.; Roozeboom, F.; Kessels, W. M. M.; Mackus, A. J. M. Area-Selective Atomic Layer Deposition of SiO_2 Using Acetylacetone as a Chemoselective Inhibitor in an ABC-Type Cycle. *ACS Nano* **2017**, *11* (9), 9303–9311.
- (48) Balasubramanyam, S.; Merkx, M. J. M.; Verheijen, M. A.; Kessels, W. M. M.; Mackus, A. J. M.; Bol, A. A. Area-Selective Atomic Layer Deposition of Two-Dimensional WS_2 Nanolayers. *ACS Materials Letters* **2020**, *2* (5), 511–518.
- (49) Merkx, M. J. M.; Sandoval, T. E.; Hausmann, D. M.; Kessels, W. M. M.; Mackus, A. J. M. Mechanism of Precursor Blocking by Acetylacetone Inhibitor Molecules during Area-Selective Atomic Layer Deposition of SiO_2 . *Chem. Mater.* **2020**, *32* (8), 3335–3345.
- (50) Yu, P.; Merkx, M. J. M.; Tezsevin, I.; Lemaire, P. C.; Hausmann, D. M.; Sandoval, T. E.; Kessels, W. M. M.; Mackus, A. J. M. Blocking mechanisms in area-selective ALD by small molecule inhibitors of different sizes: Steric shielding versus chemical passivation. *Appl. Surf. Sci.* **2024**, *665*, 160141.
- (51) Lee, J.-M.; Kim, W.-H. Area-Selective Atomic Layer Deposition of Ruthenium Thin Films by Chemo-Selective Adsorption of Short Alkylating Agents. In *2023 IEEE International Interconnect Technology Conference (IITC) and IEEE Materials for Advanced Metallization Conference (MAM)(IITC/MAM)*; IEEE, 2023; pp 1–3.
- (52) Chen, R.; Bent, S. F. Chemistry for Positive Pattern Transfer Using Area-Selective Atomic Layer Deposition. *Adv. Mater.* **2006**, *18* (8), 1086–1090.
- (53) Chen, R.; Kim, H.; McIntyre, P. C.; Bent, S. F. Investigation of Self-Assembled Monolayer Resists for Hafnium Dioxide Atomic Layer Deposition. *Chem. Mater.* **2005**, *17* (3), 536–544.
- (54) Färm, E.; Kemell, M.; Ritala, M.; Leskelä, M. Selective-area atomic layer deposition with microcontact printed self-assembled octadecyltrichlorosilane monolayers as mask layers. *Thin Solid Films* **2008**, *517* (2), 972–975.
- (55) Jiang, X.; Chen, R.; Bent, S. F. Spatial control over atomic layer deposition using microcontact-printed resists. *Surf. Coat. Technol.* **2007**, *201* (22), 8799–8807.

- (56) Jung, M.-H.; Choi, H.-S. Characterization of octadecyltrichlorosilane self-assembled monolayers on silicon (100) surface. *Korean Journal of Chemical Engineering* **2009**, *26* (6), 1778–1784.
- (57) Morsch, L.; Farmer, S.; Cunningham, K.; Sharrett, Z.; Shea, K. M. *Organic Chemistry II*; LibreTexts Publications, 2023.
- (58) Hong, J.; Porter, D. W.; Sreenivasan, R.; McIntyre, P. C.; Bent, S. F. ALD Resist Formed by Vapor-Deposited Self-Assembled Monolayers. *Langmuir* **2007**, *23* (3), 1160–1165.
- (59) Chang, C.-W.; Tseng, Y.-H.; Hsu, C.-S.; Chen, J.-T. Area-Selective Atomic Layer Deposition on Metal/Dielectric Patterns: Amphiphobic Coating, Vaporizable Inhibitors, and Regenerative Processing. *ACS Appl. Mater. Interfaces* **2023**, *15* (23), 28817–28824.
- (60) Chang, C.-W.; Hsu, H.-H.; Hsu, C.-S.; Chen, J.-T. Achieving area-selective atomic layer deposition with fluorinated self-assembled monolayers. *Journal of Materials Chemistry C* **2021**, *9* (41), 14589–14595.
- (61) Wojtecki, R.; Mettry, M.; Fine Nathel, N. F.; Friz, A.; De Silva, A.; Arellano, N.; Shobha, H. Fifteen Nanometer Resolved Patterns in Selective Area Atomic Layer Deposition—Defectivity Reduction by Monolayer Design. *ACS Appl. Mater. Interfaces* **2018**, *10* (44), 38630–38637.
- (62) Merkx, M. J. M.; Vlaanderen, S.; Faraz, T.; Verheijen, M. A.; Kessels, W. M. M.; Mackus, A. J. M. Area-Selective Atomic Layer Deposition of TiN Using Aromatic Inhibitor Molecules for Metal/Dielectric Selectivity. *Chem. Mater.* **2020**, *32* (18), 7788–7795.
- (63) Lee, S.-H.; Lee, J.-M.; Lee, J. H.; Kwak, J.; Chung, S.-W.; Kim, W.-H. Area-selective atomic layer deposition of Ru thin films using phosphonic acid self-assembled monolayers for metal/dielectric selectivity. *Mater. Lett.* **2022**, *328*, 133187.
- (64) Bent, S. F.; Kachian, J. S.; Rodriguez-Reyes, J. C. F.; Teplyakov, A. V. Tuning the reactivity of semiconductor surfaces by functionalization with amines of different basicity. *Proc. Natl. Acad. Sci. U. S. A.* **2011**, *108* (3), 956–960.
- (65) Callow, M. E.; Callow, J. A.; Ista, L. K.; Coleman, S. E.; Nolasco, A. C.; López, G. P. Use of Self-Assembled Monolayers of Different Wettabilities To Study Surface Selection and Primary Adhesion Processes of Green Algal (*Enteromorpha*) Zoospores. *Appl. Environ. Microbiol.* **2000**, *66* (8), 3249–3254.
- (66) Mao, D.; Wang, X.; Wu, Y.; Gu, Z.; Wang, C.; Tu, Y. Unexpected hydrophobicity on self-assembled monolayers terminated with two hydrophilic hydroxyl groups. *Nanoscale* **2021**, *13* (46), 19604–19609.
- (67) Liu, Y.; Jiang, L.; Wang, H.; Wang, H.; Jiao, W.; Chen, G.; Zhang, P.; Hui, D.; Jian, X. A brief review for fluorinated carbon: synthesis, properties and applications. *Nanotechnol. Rev.* **2019**, *8* (1), 573–586.
- (68) Wasserman, S. R.; Tao, Y. T.; Whitesides, G. M. Structure and reactivity of alkylsiloxane monolayers formed by reaction of alkyltrichlorosilanes on silicon substrates. *Langmuir* **1989**, *5* (4), 1074–1087.
- (69) Ulman, A. Formation and Structure of Self-Assembled Monolayers. *Chem. Rev.* **1996**, *96* (4), 1533–1554.
- (70) Xu, Y.; Musgrave, C. B. A DFT Study of the Al_2O_3 Atomic Layer Deposition on SAMs: Effect of SAM Termination. *Chem. Mater.* **2004**, *16* (4), 646–653.
- (71) Killampalli, A. S.; Ma, P. F.; Engstrom, J. R. The Reaction of Tetrakis(dimethylamido)titanium with Self-Assembled Alkyltrichlorosilane Monolayers Possessing $-\text{OH}$, $-\text{NH}_2$, and $-\text{CH}_3$ Terminal Groups. *J. Am. Chem. Soc.* **2005**, *127* (17), 6300–6310.
- (72) Dube, A.; Sharma, M.; Ma, P. F.; Engstrom, J. R. Effects of interfacial organic layers on thin film nucleation in atomic layer deposition. *Appl. Phys. Lett.* **2006**, *89* (16), 164108.
- (73) Patwardhan, S.; Cao, D. H.; Schatz, G. C.; Martinson, A. B. F. Atomic Layer Deposition Nucleation on Isolated Self-Assembled Monolayer Functional Groups: A Combined DFT and Experimental Study. *ACS Applied Energy Materials* **2019**, *2* (7), 4618–4628.
- (74) Hashemi, F. S. M.; Bent, S. F. Sequential Regeneration of Self-Assembled Monolayers for Highly Selective Atomic Layer Deposition. *Advanced Materials Interfaces* **2016**, *3* (21), 1600464.
- (75) Mameli, A.; Merkx, M. J. M.; Karasulu, B.; Roozeboom, F.; Kessels, W. M. M.; Mackus, A. J. M. Area-Selective Atomic Layer Deposition of SiO_2 Using Acetylacetone as a Chemoselective Inhibitor in an ABC-Type Cycle. *ACS Nano* **2017**, *11* (9), 9303–9311.
- (76) Minaye Hashemi, F. S.; Prasittchai, C.; Bent, S. F. Self-Correcting Process for High Quality Patterning by Atomic Layer Deposition. *ACS Nano* **2015**, *9* (9), 8710–8717.
- (77) Merkx, M. J. M.; Jongen, R. G. J.; Mameli, A.; Lemaire, P. C.; Sharma, K.; Hausmann, D. M.; Kessels, W. M. M.; Mackus, A. J. M. Insight into the removal and reapplication of small inhibitor molecules during area-selective atomic layer deposition of SiO_2 . *Journal of Vacuum Science & Technology A: Vacuum, Surfaces, and Films* **2021**, *39* (1), 0124021–0124028.
- (78) Nye, R. A.; Van Dongen, K.; de Marneffe, J. F.; Parsons, G. N.; Delabie, A. Quantified Uniformity and Selectivity of TiO_2 Films in 45-nm Half Pitch Patterns Using Area-Selective Deposition Supercycles. *Advanced Materials Interfaces* **2023**, *10* (20), 2300163–2300173.
- (79) Vallat, R.; Gassilloud, R.; Salicio, O.; El Hajjam, K.; Molas, G.; Pelissier, B.; Vallée, C. Area selective deposition of TiO_2 by intercalation of plasma etching cycles in PEALD process: A bottom up approach for the simplification of 3D integration scheme. *Journal of Vacuum Science & Technology A* **2019**, *37* (2), 020918.
- (80) Leskelä, M.; Ritala, M. Atomic layer deposition (ALD): from precursors to thin film structures. *Thin Solid Films* **2002**, *409* (1), 138–146.
- (81) Kim, J. Y.; Choi, G. H.; Kim, Y. D.; Kim, Y.; Jeon, H. Comparison of TiN Films Deposited Using Tetrakisdimethylaminotitanium and Tetrakisdiethylaminotitanium by the Atomic Layer Deposition Method. *Jpn. J. Appl. Phys.* **2003**, *42*, 4245–4248.
- (82) Chaukulkar, R. P.; Agarwal, S. Atomic layer deposition of titanium dioxide using titanium tetrachloride and titanium tetraisopropoxide as precursors. *Journal of Vacuum Science & Technology A* **2013**, *31* (3), 031509.
- (83) Jones, A. C.; Aspinall, H. C.; Chalker, P. R.; Potter, R. J.; Manning, T. D.; Loo, Y. F.; O’Kane, R.; Gaskell, J. M.; Smith, L. M. MOCVD and ALD of High-k Dielectric Oxides Using Alkoxide Precursors. *Chem. Vap. Deposition* **2006**, *12* (2–3), 83–98.
- (84) Park, B.-E.; Oh, I.-K.; Lee, C. W.; Lee, G.; Shin, Y.-H.; Lansalot-Matras, C.; Noh, W.; Kim, H.; Lee, H.-B.-R. Effects of Cl-Based Ligand Structures on Atomic Layer Deposited HfO_2 . *J. Phys. Chem. C* **2016**, *120* (11), 5958–5967.
- (85) Austin, D. Z.; Jenkins, M. A.; Allman, D.; Hose, S.; Price, D.; Dezelah, C. L.; Conley, J. F., Jr. Atomic layer deposition of ruthenium and ruthenium oxide using a zero-oxidation state precursor. *Chem. Mater.* **2017**, *29* (3), 1107–1115.
- (86) Lee, J.; Yoon, J.; Kim, H. G.; Kang, S.; Oh, W. S.; Algadi, H.; Al-Sayari, S.; Shong, B.; Kim, S. H.; Kim, H.; Lee, T.; Lee, H. B. R. Highly conductive and flexible fiber for textile electronics obtained by extremely low-temperature atomic layer deposition of Pt. *NPG Asia Materials* **2016**, *8* (11), No. e331.
- (87) Nam, T.; Lee, H.; Choi, T.; Seo, S.; Yoon, C. M.; Choi, Y.; Jeong, H.; Lingam, H. K.; Chitturi, V. R.; Korolev, A.; Ahn, J. H.; Kim, H. Low-temperature, high-growth-rate ALD of SiO_2 using amino-disilane precursor. *Appl. Surf. Sci.* **2019**, *485*, 381–390.
- (88) Oh, I.-K.; Park, B.-E.; Seo, S.; Yeo, B. C.; Tanskanen, J.; Lee, H.-B.-R.; Kim, W.-H.; Kim, H. Comparative study of the growth characteristics and electrical properties of atomic-layer-deposited HfO_2 films obtained from metal halide and amide precursors. *Journal of Materials Chemistry C* **2018**, *6* (27), 7367–7376.
- (89) Oh, I.-K.; Sandoval, T. E.; Liu, T.-L.; Richey, N. E.; Nguyen, C. T.; Gu, B.; Lee, H.-B.-R.; Tonner-Zech, R.; Bent, S. F. Elucidating the Reaction Mechanism of Atomic Layer Deposition of Al_2O_3 with a Series of $\text{Al}(\text{CH}_3)_x\text{Cl}_{3-x}$ and $\text{Al}(\text{C}_y\text{H}_{2y+1})_3$ Precursors. *J. Am. Chem. Soc.* **2022**, *144* (26), 11757–11766.
- (90) Kim, M.; Kim, J.; Kwon, S.; Lee, S. H.; Eom, H.; Shong, B. Theoretical Design Strategies for Area-Selective Atomic Layer Deposition. *Chem. Mater.* **2024**, *36* (11), 5313–5324.

- (91) Kim, H. G.; Kim, M.; Gu, B.; Khan, M. R.; Ko, B. G.; Yasmeen, S.; Kim, C. S.; Kwon, S.-H.; Kim, J.; Kwon, J.; Jin, K.; Cho, B.; Chun, J. S.; Shong, B.; Lee, H.-B.-R. Effects of Al Precursors on Deposition Selectivity of Atomic Layer Deposition of Al_2O_3 Using Ethanethiol Inhibitor. *Chem. Mater.* **2020**, *32* (20), 8921–8929.
- (92) Yarbrough, J.; Bent, S. F. Area-Selective Deposition by Cyclic Adsorption and Removal of 1-Nitropropane. *J. Phys. Chem. A* **2023**, *127* (37), 7858–7868.
- (93) Maue, P.; Chantraine, É.; Pieck, F.; Tonner-Zech, R. Accurately computed dimerization fraction of ALD precursors and their impact on surface reactivity in area-selective atomic layer deposition. *ChemRxiv* **2024**, DOI: [10.26434/chemrxiv-2024-x3n3k](https://doi.org/10.26434/chemrxiv-2024-x3n3k).
- (94) Merkx, M. J. M.; Angelidis, A.; Mameli, A.; Li, J.; Lemaire, P. C.; Sharma, K.; Hausmann, D. M.; Kessels, W. M. M.; Sandoval, T. E.; MacKus, A. J. M. Relation between Reactive Surface Sites and Precursor Choice for Area-Selective Atomic Layer Deposition Using Small Molecule Inhibitors. *J. Phys. Chem. C* **2022**, *126*, 4845–4853.
- (95) Soethoudt, J.; Tomczak, Y.; Meynaerts, B.; Chan, B. T.; Delabie, A. Insight into Selective Surface Reactions of Dimethylamino-trimethylsilane for Area-Selective Deposition of Metal, Nitride, and Oxide. *J. Phys. Chem. C* **2020**, *124* (13), 7163–7173.
- (96) Liu, T. L.; Bent, S. F. Copper Oxidation Improves Dodecanethiol Blocking Ability in Area-Selective Atomic Layer Deposition. *Advanced Materials Interfaces* **2022**, *9* (19), 2200587.
- (97) Mori, Y.; Cheon, T.; Kotsugi, Y.; Kim, Y. H.; Park, Y.; Ansari, M. Z.; Mohapatra, D.; Jang, Y.; Bae, J. S.; Kwon, W.; Kim, G.; Park, Y.; Lee, H. B.; Song, W.; Kim, S. H. Self-Formation of a Ru/ZnO Multifunctional Bilayer for the Next-Generation Interconnect Technology via Area-Selective Atomic Layer Deposition. *Small* **2023**, *19* (34), 2300290.